Universidade de Aveiro Departamento de Biologia

Ano 2018

Bruno
Carvalho Ramos

Characterization of *Staphylococcus aureus*-mediated inhibition of IAV-induced type I IFN signalling

Caracterização da inibição mediada por *Staphylococcus aureus* da sinalização via IFN tipo I induzida pelo vírus influenza A

DECLARAÇÃO

Declaro que este relatório é integralmente da minha autoria, estando devidamente referenciadas as fontes e obras consultadas, bem como identificadas de modo claro as citações dessas obras. Não contém, por isso, qualquer tipo de plágio quer de textos publicados, qualquer que seja o meio dessa publicação, incluindo meios eletrónicos, quer de trabalhos académicos.

Universidade de Aveiro

Departamento de Biologia

Ano 2018

Bruno Carvalho Ramos

Characterization of *Staphylococcus aureus*-mediated inhibition of IAV-induced type I IFN signalling

Caracterização da inibição mediada por *Staphylococcus aureus* da sinalização via IFN tipo I induzida pelo vírus influenza A

Dissertação apresentada à Universidade de Aveiro para cumprimento dos requisitos necessários à obtenção do grau de Mestre em Microbiologia, realizada sob a orientação científica da Doutora Sónia Mendo, Professora auxiliar com agregação do Departamento de Biologia da Universidade de Aveiro e co-orientação da Doutora Christina Ehrhardt, Investigadora Principal do Instituto de Virologia de Münster

o júri

presidente	Doutor Artur Jorge da Costa Peixoto Alves equiparado a Investigador Principal da Universidade de Aveiro
vogal - arguente principal	Doutora Daniela Maria Oliveira Gandra Ribeiro bolseira de pós-doutoramento da Universidade de Aveiro
vogal - orientador	Professora Doutora Sónia Alexandra Leite Velho Mendo Barroso professora auxiliar com agregação da Universidade de Aveiro

agradecimentos

Em primeiro lugar, gostaria de agradecer especialmente à PD Dra. Christina Ehrhardt por toda a ajuda e apoio desde o primeiro dia. Sempre seguiu e considerou o meu trabalho e bem-estar, contribuindo para um aluno alegre e motivado. Após guiar-me neste cativante projeto com conhecimentos esclarecedores e questões pertinentes, só posso estar agradecido pela oportunidade de trabalhar consigo. Por fim, um muito obrigado pela chance de fazer parte do Instituto de Virologia de Münster.

Naturalmente, também gostaria de expressar a minha gratidão ao Prof. Dr. Stephan Ludwig e ao IVM por receber-me e proporcionar tudo o que foi necessário para um trabalho tranquilo.

Queria também aproveitar esta ocasião para agradecer à Anmari, Carolin, Christin e Andre por todo o suporte no trabalho laboratorial, assim como os conselhos dados na preparação do mesmo. Vocês sempre tiveram a preocupação de assegurar que eu entendia os vários procedimentos e que os realizava de maneira correta.

De seguida, quero agradecer a todas as pessoas incríveis que conheci no IVM, as quais me ajudaram e mostraram uma disponibilidade imediata com todas as minhas dúvidas e problemas. Estou também grato pelos conselhos e *feedback* recebido nos seminários realizados que inspiraram novas ideias e visões para o meu trabalho. Vocês proporcionaram um ambiente divertido e saudável que resultou em grandes amizades, as quais irão permanecer para a vida.

Por último, não esquecer a minha família e amigos que me incentivaram desde Portugal a desfrutar do tempo e experiências ao longo do ano, bem como o apoio da Prof. Dra. Sónia Mendo e todos os professores durante os últimos dois anos na Universidade de Aveiro.

acknowledgements

Firstly, I want to especially thank Dr. Christina Ehrhardt for all the help and support since the initial day. You always looked after my work and well-being, thus contributing to a motivated and happy student. By guiding me through this exciting project with insightful information and critical questioning, I can only be grateful for the opportunity to research and work with you. At last, thank you for the stimulating chance of being part of the Institute of Virology Münster.

Naturally, I would also like to express my gratitude to Dr. Stephan Ludwig and the IVM for receiving me and providing everything I needed for a serene work.

I would also like to take this occasion to thank Anmari, Carolin, Christin and Andre for all the assistance in the laboratory as well as the guidance on the experiments preparation. You always cared and did your best to assure I understood the purpose of several procedures and worked in a proper way.

Next, I want to thank all the amazing people I met at the IVM, which helped me with my doubts and showed a prompt availability when I needed. I am also thankful for the advice and feedback I received at the seminars that inspired new ideas and views for my work. You provided a fun and healthy environment that allowed me to make great friends, who will remain for life.

Not to forget are my family and friends who have encouraged me from back home to savour the time and experiences throughout the year as well as the support of Dr. Sónia Mendo and all the other teachers during this last two years at Universidade de Aveiro.

resumo

A cooperação viral e bacteriana, durante o curso de infeção do trato respiratório inferior, revela-se uma ameaça preocupante para a saúde pública, sendo uma das maiores causas de mortalidade à escala global. O vírus Influenza A e *Staphylococcus aureus* (*S. aureus*) estão entre os mais comuns exemplos e, considerando os problemas atuais com estirpes de *S. aureus* multi-resistentes a antibióticos de última linha, co-infeções são uma grande preocupação da medicina atual. Dado que ambos os patogénicos manipulam certas vias de sinalização celular com vista aos seus próprios objetivos de internalização, replicação, assim como, evasão do sistema imunitário, estas cascatas moleculares são amplamente estudadas para desvendar novas soluções terapêuticas. A escolha desta abordagem previne a ação direta nos patogénicos e, consequentemente, a acumulação de resistências que suscitam complicações e um círculo vicioso na investigação médica.

Neste trabalho, foi demonstrado que a capacidade de *S. aureus* inibir a via JAK-STAT depende da estirpe utilizada, visto que não se verificou qualquer efeito provocado por *S. aureus* LS1. Em sentido oposto, *S. aureus* SH1000 apresenta uma eficácia similar à estirpe *S. aureus* 6850 na inibição da sinalização mediada via IFN tipo I. Inclusivamente, além de *S. aureus* SH1000 wt, um impacto semelhante deste mecanismo foi revelado por diversos mutantes. Um dos mutantes (Δ*agr*), que diferem na expressão de importantes reguladores de virulência da bactéria, assinala um efeito ainda mais acentuado na transcrição de genes estimulados pelo IFN. Estes dados são suportados por um bloqueio quase total da dimerização entre STAT1 e STAT2. Além disso, uma eficácia de internalização contrastante das estirpes mutantes *S. aureus* SH1000 Δ*sigB*, Δ*agr*, Δ*sarA* and Δ*agr*+Δ*sarA* em relação à estirpe *S. aureus* SH1000 wt é notória. No entanto, é possível compreender que a capacidade inferior de infetar as células por parte dos mutantes não afeta a sua capacidade de inibir a resposta do sistema imunitário.

Em última análise, este trabalho permite traçar um caminho para futuros projetos à medida que a hipótese de uma inibição mediada por toxinas de *S. aureus* fica enfraquecida e a conjetura de o efeito ser provocado por uma proteína estrutural bacteriana é fortalecida. Com os dados obtidos, uma futura junção com métodos mais sensíveis e precisos, como a espectrometria de massa baseada na proteómica, possibilitará alcançar resultados mais conclusivos.

abstract

Viral and bacterial infections act in concert, when both are present in the lower respiratory tract. This cooperation turns them into a bigger threat and, consequently, one of the highest causes of global mortality. Influenza A viruses (IAV) and *Staphylococcus aureus* (*S. aureus*) are among the most common examples and considering the nowadays problematic multi-drug-resistant *S. aureus* strains, co-infections are a major medical concern. Since both pathogens manipulate certain cellular signalling pathways for own purposes during internalisation, replication or to elude the immune system, these molecular cascades are widely studied to unravel new therapeutic approaches. Targeting cellular factors will prevent the direct action on the pathogens and avoid resistances build-up, which brings future complications and a "loop" in medicine research.

Within the present work, it could be shown that *S. aureus* capacity to inhibit the JAK-STAT pathway depends on the challenged strain as we clearly saw no effect provoked by *S. aureus* LS1. On the contrary, *S. aureus* SH1000 reveals similar effectiveness on the inhibition of type I IFN-mediated signalling to the *S. aureus* 6850 strain. As a matter of fact, not only *S. aureus* SH1000 wt strain displayed this mechanism but also several mutants, which differed in expression of important virulence regulators of the bacteria. Additionally, one of the mutants (Δ*agr*) presents a more impactful outcome on the interferon stimulated gene (ISG) transcription, which is supported by an almost total impairment of the STAT1-STAT2 dimerization. Moreover, we also show contrasting internalisation efficacy of the *S. aureus* SH1000 Δ*sigB*, Δ*agr*, Δ*sarA* and Δ*agr*+Δ*sarA* mutant strains in comparison to the *S. aureus* SH1000 wt strain. However, as it's possible to acknowledge their inferior capacity to infect, their ability to cause immune response inhibition doesn't get affected.

Ultimately, we pave the way for the next research studies as the hypothesis of a *S. aureus* toxin-mediated inhibition is weakened and a bacterial structural protein premise is strengthened. Ultimately, with the data we detain on this subject, a future pairing with more sensitive and precise methods, such as mass spectrometry-based proteomics, will provide more conclusive results.

Table of contents

List of figures IV

1. Introduction 1

1.1 Influenza A virus 2

1.1.1 Morphology and replication cycle 2

1.1.2 Clinical Picture 6

1.2 Staphylococcus aureus 6

1.2.1 Structure 7

1.2.2 Virulence Factors 8

1.2.3 Clinical Relevance 9

1.3 Co-infection with IAV and *S. aureus* 10

1.3.1 Epidemiology 10

1.3.2 Co-pathogenesis 11

1.4 Inflammatory Response 12

1.4.1 Pro-Inflammatory cytokines and chemokines 12

1.4.2 JAK-STAT pathway 14

1.4.3 Immune response after IAV infection 15

1.4.4 Immune response after *S. aureus* infection 16

1.5 Objective 16

2. Material 18

2.1 Used Devices 18

2.2 Chemicals 18

2.3 Cell culture material 19

2.4 RNA work material 19

2.4.1 Primers for human probes 20

2.5 Cell lines 20

2.6 Pathogens 20
2.6.1 IAV strains 20
2.6.2 *S. aureus* strains 20
2.7 Media and buffers 21
2.8 Antibodies 24
3. Methods 26
3.1 Cell Culture Techniques 26
3.2 Virological Methods 26
3.2.1 Virus Growth 26
3.2.2 Determination of infectious virus particles - plaque assay 26
3.3 Bacteriological Methods 27
3.3.1 Cultivation, preservation and inactivation of prokaryotic cells 27
3.3.2 Determination of bacterial titres 27
3.4 Co-infection Model 27
3.4.1 Co-infection in vitro 27
3.5 Stimulation of eukaryotic cells 28
3.6 Protein work 28
3.6.1 Production of protein extracts 28
3.6.2 SDS polyacrylamide gel electrophoresis (SDS-Page) 28
3.6.3 Western Blot 29
3.6.4 Co-Immunoprecipitation (Co-IP) 29
3.7 RNA work 30
3.7.1 RNA isolation using RNeasy Kit (Qiagen) 30
3.7.2 Reverse transcription of RNA (cDNA synthesis) 30
3.7.3 Quantitative Real-Time PCR (qRT-PCR) 31
4. Results 32
4.1 The type I IFN-mediated signalling is blocked in presence of *S. aureus* infection 32

4.2 *S. aureus* SH1000 wild-type and mutant strains present different growth behaviour and contrasting capacity to infect 36

4.3 STAT1 phosphorylation is still inhibited upon adjustment of infection doses of bacterial mutants in co-infection scenario 38

4.4 IAV replication is increased in the presence of *S. aureus* SH1000 39

4.5 Type I IFN-mediated ISG mRNA expression is reduced upon *S. aureus* co-infection 40

5. Discussion 43

5.1 *S. aureus*-mediated inhibition of type I IFN signalling seems to be strain-dependent 43

5.2 *Agr* silence results in a reduction of IAV-induced immune response 44

5.3 Bacterial load doesn't correlate to the block of immune responses 45

5.4 Perspectives on the elucidation of *S. aureus*-mediated interference with STAT1-STAT2 dimerization 47

6. Bibliography 50

List of figures

Fig. 1. Influenza A virus (IAV) virion 3
Fig. 2. Schematic diagram of the IAV life cycle 5
Fig. 3. Schematic representation of the *S. aureus* structure [adapted from [83]] 8
Fig. 4. Scheme of type I IFN-dependent signalling and ISGF3-mediated gene expression. 15
Fig. 5. Protein expression and virus titres resultant of IAV co-infection with *S. aureus* 6850 33
Fig. 6. Protein expression resultant of IAV co-infection or IFNβ co-stimulation with different strains of *S. aureus* (6850 wt, SH1000 wt and mutants (Δ*sigB*, Δ*agr*, Δ*sarA*, Δ*agr*+Δ*sarA*), LS1 wt (Δ*sigB*, Δ*agr*, Δ*sarA*, Δ*agr*+Δ*sarA*)) 34
Fig. 7. STAT1-STAT2 dimerization status following a IFNβ co-stimulation with *S. aureus* SH1000 wt and mutants (Δ*sigB*, Δ*agr*) 35
Fig. 8. Growth kinetics of *S. aureus* wt and mutants (Δ*sigB*, Δ*agr*, Δ*sarA*, Δ*agr*+Δ*sarA*) 36
Fig. 9. Bacterial titres of *S. aureus* wt and mutants (Δ*sigB*, Δ*agr*, Δ*sarA*, Δ*agr*+Δ*sarA*) overnight culture 37
Fig. 10. Invasiveness of *S. aureus* SH1000 wt and mutants (Δ*sigB*, Δ*agr*, Δ*sarA*, Δ*agr*+Δ*sarA*) 38
Fig. 11. Protein expression resultant of IAV co-infection with *S. aureus* SH1000 wt and mutants (Δ*sigB*, Δ*agr*, Δ*sarA*, Δ*agr*+Δ*sarA*) 39
Fig. 12. Virus replication resultant of IAV co-infection with *S. aureus* SH1000 wt and mutants (Δ*sigB*, Δ*agr*, Δ*sarA*, Δ*agr*+Δ*sarA*) 40
Fig. 13. mRNA levels of IFNβ and ISGs following a IAV co-infection with *S. aureus* 6850 and *S. aureus* SH1000 wt and mutants (Δ*sigB*, Δ*agr*) 41

1. Introduction

"Polymicrobial diseases involve two or more microorganisms that act synergistically, or in succession, to mediate complex disease processes" [1].

Influenza A virus (IAV) and bacterial pneumonia played a great role in one of the most relentless pandemics of the twentieth century. The "Spanish flu" of 1918 is considered by some as the mother of all pandemics and 95% of the mortality was accredited to bacterial co-infection [2]. 1957 Asian flu and 1968 Hong Kong flu pandemics were other remarkable events in the painful path engraved by IAV and bacteria. Less severe death rates but more *Staphylococcus aureus* (*S. aureus*) incidence in these two last dates may expose then the increased use of antibiotics and the emergence of drug-resistant bacteria [3,4]. Nowadays, preventing infections with methicillin-resistant *S. aureus* (MRSA) has become a vital part and one of the major concerns of hospital care, highlighting the necessity for methodical control of anti-bacterial medication and catalysing the pursuit for alternate approaches. Preparation for future pandemics should then be looked at as of high relevance given the death tolls chronicled in previous happenings and antibiotics as well as pneumococcal vaccines ought to be stashed in precaution [5].

At the present time, the majority of available antimicrobial agents against staphylococci exert their bactericidal or bacteriostatic effects by a limited number of mechanisms. In fact, all current first-line and second-line therapies [6] against *S. aureus*, both MRSA and methicillin-sensitive *S. aureus* (MSSA), exert their antimicrobial effect via one of three mechanisms: disruption of the cell wall and/or cell membrane (β-lactams, glycopeptides, lipopeptides), ribosome-targeted interference of protein synthesis (tetracyclines, macrolides, lincosamides, oxazolidinones), or inhibition of nucleotide production by disrupting folate synthesis (trimethoprim-sulfamethoxazole [TMP-SMX]) [7]. However, bacteria are rapidly developing resistances to used therapeutics, which ended becoming almost obsolete [8]. It is then urgent to find solutions to improve patient outcomes and to better manage possible dangerous situations on health care environments [9].

Regarding IAV and accordingly to the World Health Organization (WHO), the hemagglutinin (HA) protein is the present target for the currently licensed seasonal influenza vaccines, which have to be re-evaluated each year due to the antigenic drift of the circulating strain. The protection level that these vaccines offer is not ideal and manufacturing time is far from being swift. If possible, new vaccines should thus widen the current coverage to contain antigenically different viruses and thus to improve immune response [10].

In general, *S. aureus* and IAV has evolved a prosperity of varied strategies to evade natural host defences. For the invasion and persistence success, an efficient evasion of both innate and adaptive immune system is of extreme importance. To better understand the pathogen-mediated mechanisms in their cooperative infective process, this work will mainly focus on these two health relevant pathogens: IAV and *S. aureus* (*S. aureus*), both important pathogens of the respiratory tract. This knowledge is mandatory to estimate pathogenicity and outcome of infections as well as the identification of novel targets for antipathogen therapies.

1.1 Influenza A virus

Influenza A viruses (IAV) belong to the *Orthomyxoviridae* family of viruses. This family is also constituted by Influenza B (IBV), C (ICV) and D viruses (IDV) as well as *Thogotovirus* and *Isavirus* [11–14]. The three genera of influenza differ both in their pathogenicity and in virus particle assembly. In contrast to IBV, ICV and IDV, IAV has a very broad host range including various species of birds and several mammals. However, wild birds and waterfowl are considered as the main reservoir and primary host [15]. While strains of all subtypes of influenza A virus are isolated from these organisms, disease is uncommon. Nevertheless, IAV still represent a severe threat to mankind and are among the most dangerous respiratory pathogens. With 3–5 million hospitalizations and up to 650 000 fatalities annually, as estimated by a study conducted by the United States Centers for Disease Control and Prevention (US-CDC) [16], these viruses are not only a devastating burden to global health but also significantly impact the economy. Death rates, as those mentioned, follow a cyclic pattern, which fluctuates with seasonal changes in humidity. These vicissitudes occur when novel mutations are introduced by the error-prone viral polymerase. More distinct variations in pathogenicity mostly arise when two viruses trade RNA-segments, hence creating a hybrid (reassorted) strain with different virulence attributes, or once a zoonotic virus starts replicating in human hosts [17]. It's also worrisome that the current prevention strategies seem uncapable to reduce this problem and show imperfections, which prove to be fatal every year. Therefore, priority to IAV will be given in the next chapters.

1.1.1 Morphology and replication cycle

IAV is an enveloped RNA virus with a segmented negative single-stranded genome. It is distinguished from IBV, ICV and IDV through its nucleoprotein (NP) and matrix protein (M1), which are major structural components of its virions, structures that possess a lipid envelope derived from the host cellular membrane during the budding [18,19]. They are mostly pleomorphic with an average size of 80 to 120 nm in diameter, but several micrometres-sized filamentous structures can be

detected. Inside the particle are eight genome segments that encode the viral proteins [20,21]. Each segment is covered with NPs and associated with the viral polymerase that is consisted of the following subunits: polymerase basic protein 1 (PB1), 2 (PB2) and polymerase acid protein (PA) (Fig.1). These viral proteins together with the viral RNA (vRNP) form the viral ribonucleoprotein (vRNP) complexes [22–25]. In the virion envelope the surface proteins hemagglutinin (HA) [26] and neuraminidase (NA) [27] as well as the proton channel (M2) [28] are embedded [29] (Fig.1). For HA and NA, 16 and 9 different subtypes have been described so far [30], even though two influenza-like viral genomes (H17N10 and H18N11) were detected in bats [31]. In the interior part of the envelope, the virion morphology is maintained by the action of M1 [32,33]. Further non-structural (NS) proteins that play a role during virus replication are encoded in the genome of IAV. The best described is NS1, which is synthesized by all known virus strains upon infection but detected in small amounts of the virions [34]. NS1 is a multifunctional protein whose main role is to block the host's antiviral immune response [35,36]. NS2 (NEP), another non-structural protein is responsible for the export of RNP [37]. Besides the last ones referred, there is expression of other NS proteins in a virus strain-specific way [38].

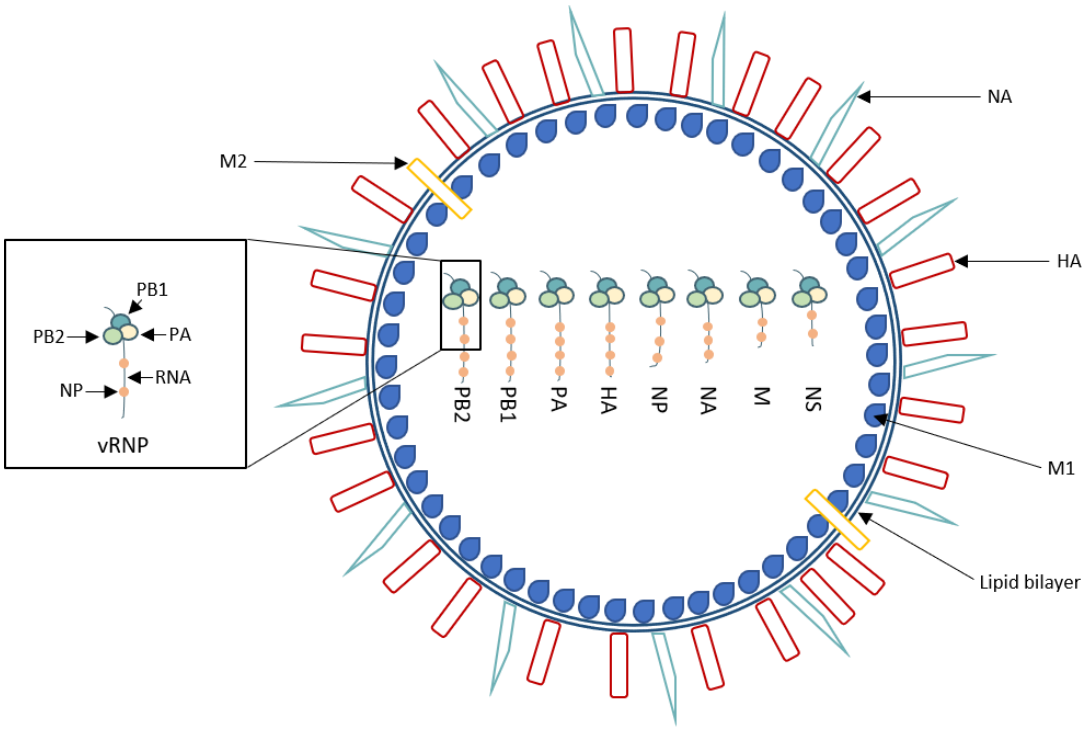

Fig. 1. Influenza A virus (IAV) virion. An IAV particle is surrounded by a lipid bi-layer structure, containing two surface viral glycoproteins, hemagglutinin (HA) and neuraminidase (NA) and the M2 ion-channel protein. Under the viral lipid bilayer, the matrix (M1) protein is present, which associates with both ribonucleoprotein and the viral envelope. Underneath, the core of the virus made of eight viral RNA segments that are encapsidated by the viral nucleoprotein (NP). Each one of the

formed vRNPs is associated with the viral polymerase complex, which is comprised of three polymerase sub-units: PB1, PB2 and PA.

Viral replication starts with the attachment of the virus to terminal N-acetylneuraminic acids (sialic acids) on the host surface (Fig. 2). HA of avian virus isolates have high specificity for α (2,3)-glycosidic galactose-linked sialic acids as found on the intestinal epithelium of birds, while human virus isolates preferentially bind to α (2,6)-linked sialic acids, which are predominantly present on the upper human respiratory epithelium [39]. After receptor-mediated endocytosis, the pH in the endosome decreases, followed by a conformational change of the HA, which in turn ends up in the fusion of the viral and endosomal membrane. The vRNPs are released into the cytosol, at the same time M1 dissolves, so that the nuclear localization signals of the vRNPs are released. The M1 protein is then imported into the nucleus separately [40]. Afterwards, the trimeric viral polymerase complex catalyses the replication and transcription of the IAV genomic RNAs in the nucleus [41,42]. Viral RNA replication starts with the synthesis of a positive-sense copy of the vRNA, termed complementary RNA (cRNA) [43]. After that, this cRNA is copied to produce large amounts of vRNA [11,44]. Viral RNA transcription is initiated by the binding of PB2 to the 5'-cap structure of host mRNAs [45–47]. The endonuclease activity of PA then 'snatches' the cap structure and the 10–13 nucleotides included with the cap serve as a primer for viral mRNA synthesis [48]. This cap-snatching mechanism is also important for the cytosolic translation by cellular ribosomes and may deplete or limit the host cell protein synthesis.

Viral protein synthesis takes place in two phases. First, the early proteins NP, NS1 and the polymerase subunits are expressed, followed by synthesis of the other structural proteins [49]. The glycoproteins HA and NA as well as M2 are synthesized at the endoplasmic reticulum, modified and subsequently transported to the host cell surface [50,51]. After their synthesis in the cytoplasm, the viral polymerase subunit proteins and NP are imported into the nucleus via their nuclear localization signals [43,52–54] to catalyse the replication and transcription of vRNA. In second place, the late M1 [55], NEP/NS2 [56], and NS1 [57] proteins are imported into the nucleus to execute their roles in vRNP nuclear export (M1 and NEP/NS2), while NS1 protein is thought to play a part in the processing and export of viral mRNAs [58].

The nuclear export of newly synthesized vRNP complexes requires the viral NEP/NS2 and M1 proteins. The latter is believed to create an association between vRNPs and NEP/NS2. M1 connection with vRNP might require M1 SUMOylation, which appears to shield M1 from proteasomes and supports the vRNP export [59]. This shift in protein function is due to a shift from

ubiquitinated to SUMOylated M1 at lysine 242 during the viral life cycle [60]. Intriguingly, it is initiated by a tumour suppressor AIMP2 that binds to NEP, gets stabilized, and functions as positive regulator of IAV replication [61]. In turn, at the plasma membrane, HA and NA (the two surface spike glycoproteins) interact with lipid rafts, at the budding sites of influenza virus [62]. Segment-specific packaging signals are necessary for the assembly and virion incorporation of the eight vRNPs. M1 [63], due to the interaction with lipid membranes, vRNPs and NEP/NS2 is essential in the assembly and packaging processes as well as the M2 protein [64], which have the cytoplasmic tail that mediates vRNP incorporation. M2, which is found in the raft periphery, appears to mediate membrane scission and particle release [65]. Finally, the enzymatic activity of viral NA splits off terminal sialic acids on the virions and the host cell to prevent accumulation of newly synthesized viruses and re-infection of already infected cells [66].

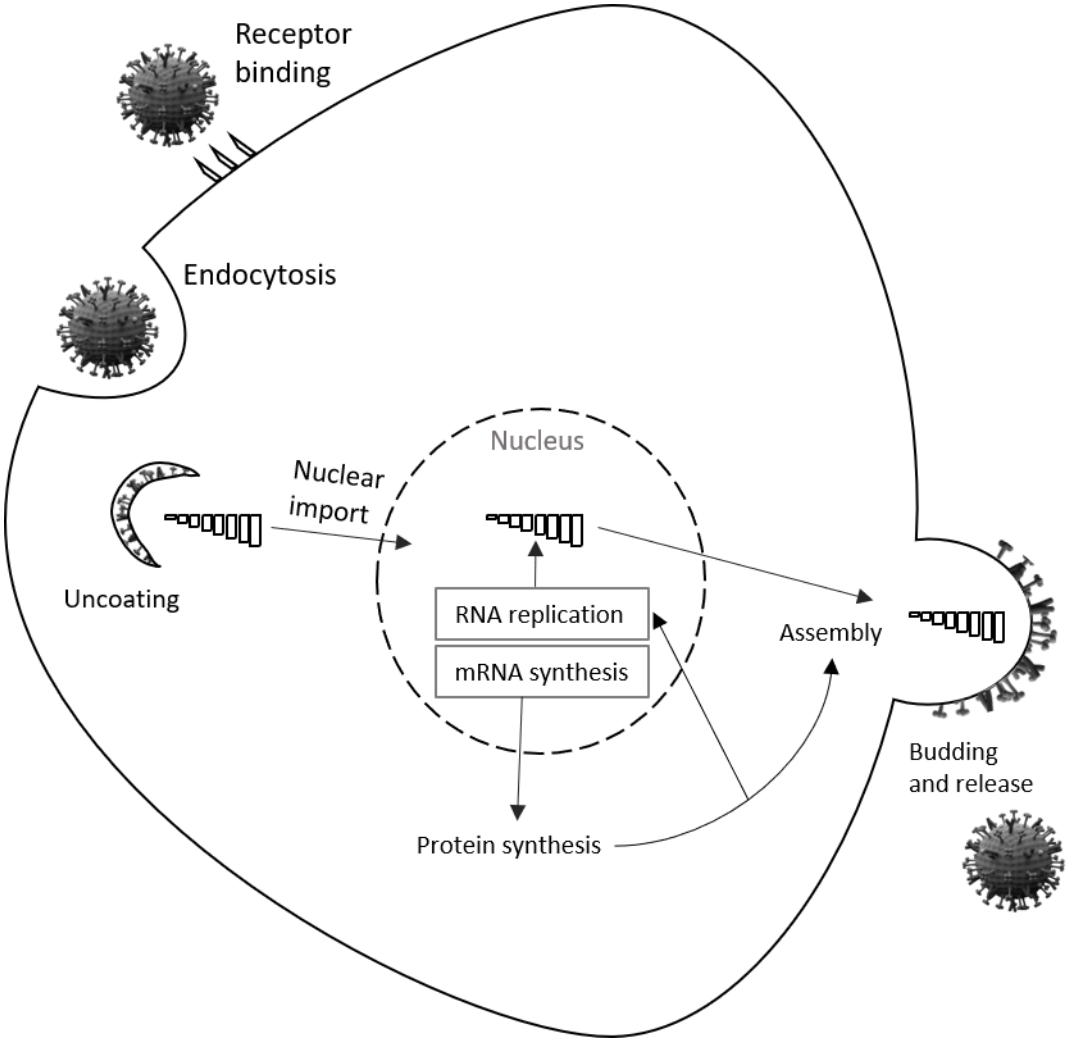

Fig. 2. Schematic diagram of the IAV life cycle. IAV infection initiates by binding of the virus to sialylated host cell receptors and posterior endocytosis-mediated entry. The release of vRNPs into the cytoplasm is then enabled by fusion of viral and

endosomal membranes at low pH. Subsequently, the transport of the segmented viral genome to the nucleus occurs, where replication and transcription take place. Afterwards, the protein synthesis occurs in the cytoplasm. Early proteins are translocated back to the nucleus for replication and transcription purposes. Late proteins are extremely important for the export of vRNPs accumulated in the nucleus. The assembly and budding of progeny virions is carried out at the cell membrane until release into the extracellular fluid.

1.1.2 Clinical Picture

As causative agent of the so-known classic flu, its transmission is usually achieved by droplet infection from person to person and begins in the upper respiratory tract [67,68]. The typical symptoms range from high fever to body aches after a short incubation period. Most people recover after one or two weeks without complications that are normally reserved for the elderly, pregnant and newborns, who are at a higher risk of secondary bacterial pneumonia, for instance [69].

IAV shedding is predominant in the 24-48h time period after illness onset, declining vertiginously in the following days to almost undetectable levels at days 6-7. This suggests a close match between clinical disease dynamics and seasonal as well as pandemic viral shedding magnitude, facilitating the use of profiles to predict the illness and infectiousness in a clinical matter [70,71].

Vaccination is currently the best available protection against influenza virus infection, but it has to be renewed annually as the surface proteins HA and NA change continuously due to the antigen drift feature [10]. These continuous variations also result in the annual influenza epidemics, which typically occur during the winter season. Another risk potential of the IAV is based on the sudden appearance of new antigens that have potential to cause a pandemic. Because of the segmented genome and exchange of its segments, the so-called antigenic shift, during infection with more than one virus subtype (reassortment) might occur [72]. The newly emerged subtypes contain the characteristics of the parent strains in a new combination leading to non-existent immunity in naive hosts [73].

1.2 Staphylococcus aureus

S. aureus is a globular, gram-positive bacterium that belongs to the family of *Staphylococcaceae* [74–76]. It is a facultative anaerobe bacterium that forms golden yellow pigments and presents coagulase and haemolysis-positive tests [77–79]. Carried by 10-35% of children and by ~35% of adult population, *S. aureus* can exploit a breach in a weakened host immune system to cause pneumonia that accounts for 20–30% of nosocomial infections. In addition, *S. aureus* also remains to be one of the leading causes of death during influenza epidemics [80,81]. Further, a high prevalence of community-

acquired pneumonia throughout high influenza activity instigated by multidrug resistance strains of *S. aureus* among otherwise healthy individuals is observed [81,82].

1.2.1 Structure

Most staphylococci possess a capsule of polysaccharides, which prevents phagocytosis by immune cells and thus increases the virulence. So far, at least 18 different serotypes have been described, but most infections are caused by the serotypes five and eight [83]. They differ mostly by their capsule polysaccharide composition, sugar linkages and sites of acetylation. Nevertheless, they present variances in some biological properties, which will naturally affect their virulence [84]. The outer bacterial cell wall consists mainly of peptidoglycans (PGN), which harbour alternating subunits of N-acetylglucosamine and N-acetylmuramic. The cell wall bound teichoic acids (WTA) are composed of a polymer of ribitol phosphate and N-acetylglucosamine [85]. In addition, *S. aureus* forms lipoteichoic acids (LTA), which consist of glycerophosphate units and are anchored to the cell membrane [86] (Fig. 3). In addition, the penicillin-binding protein (PBP) enzyme, which is part of the cell wall, supports the last step of PGN synthesis and represents a target for β-lactam antibiotics [87] (Fig. 3). *S. aureus* produces a variety of enzymes, toxins and other factors that increase virulence. These include several microbial surface components recognizing adhesive matrix molecules (MSCRAMM) that mediate binding to the extracellular matrix of the host [88]. For the supply of nutrients various lipases, nucleases, proteinases and collagenases are expressed. Other toxins, e.g. α-hemolysin [89] and Panton-Valentine leukocidin (PVL) [90], lyse erythrocytes and leukocytes, respectively. Additional ones are attributed to the fumed superantigens, examples of which are Toxic shock syndrome toxin-1 (TSST-1) [91] as well as Enterotoxins A (SEA) and B (SEB) [92], that are secreted into the surrounding tissue.

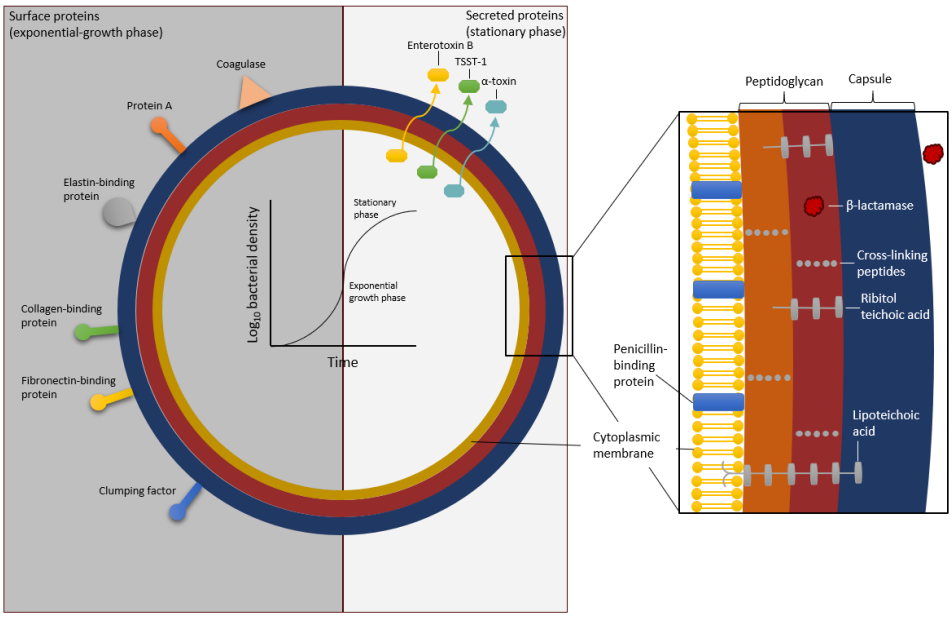

Fig. 3. Schematic representation of the *S. aureus* structure [adapted from [83]]. Surface and secreted proteins are shown. The production of bacterial proteins is dependent on the bacterial growth phase, which is depicted in the centre of the bacterium.

1.2.2 Virulence Factors

Bacteria initiate the invasion process by adhering to host cell membranes via the expression of adhesins. As invasion of host cells is equally effective with live and killed bacteria, besides a microbial pathogenicity mechanism, a strategy of the host defence system has to be considered [93]. After host cell invasion, diverse post-invasion events are possible: the intracellular metabolically active bacteria can induce host cell immune system activation and death. A longer persistence is also feasible by downregulation of cytotoxins, which allows a formation of a bacterial pool for chronic infections. These effects cannot be attributed to a single virulence factor but are most likely induced by the action of different bacterial components. Specially, α-toxin and gene products regulated by the accessory gene regulator (*agr*) and the alternative sigma factor B (sigB) seem to have relevant roles [94]. *Agr* and sigB are both strongly linked to those two opposite post-invasion outcomes mentioned above, respectively.

During acute infection, *S. aureus* require the simultaneous action of the *agr* and the accessory regulatory (*sarA*) loci to defend against invading immune cells by causing inflammation and cytotoxicity and to escape from phagosomes in their host cells that enable them to settle an infection at high bacterial density [95]. To persist intracellularly the bacteria subsequently need to silence *agr* and *sarA*. Indeed, *agr* and *sarA* deletion mutants expressed a much lower number of

virulence factors and could survive at high numbers within the cells. SigB plays a crucial function to promote bacterial intracellular persistence since, in the chronic stage of infection, it downregulates the aggressive bacterial phenotype and mediates the formation of dynamic Small Colony Variants (SCV)-phenotypes [95]. Thereby, SigB-dependent gene expression is distinctly linked to the stationary phase [96,97].

In addition, the *agr*-dependent system enables the quorum-sensing ability in staphylococci and leads to genetic adaptation in response to different stimuli. Depending on cell density, toxin production is affected and, thus, the disease development [98]. SigB has, likewise, a central role on the dynamic adjustments during infection for an efficient biofilm maturation, if needed. Moreover, a report revealed some findings that propose SigB as operating upstream of the *agr* quorum-sensing system, in response to environmental signals [99].

1.2.3 Clinical Relevance

S. aureus is both a commensal bacterium and a major human pathogen that causes a wide range of clinical infections [8,83,100]. It is a leading cause of bacteremia and infective endocarditis as well as osteoarticular, skin and soft tissue, pleuropulmonary, and device-related infections [6,8,101]. About one third of the total population is permanently colonized with *S. aureus* [102] and the past two decades have witnessed two clear shifts in the epidemiology of *S. aureus* infections: first, a growing number of health care associated infections and second, an epidemic of community-associated skin and soft tissue infections driven by strains with certain virulence factors and resistance to β-lactam antibiotics [103,104]. Livestock and domestic animals have also been colonized with *S. aureus*, where it plays an important economic role, especially as cause of mastitis [105].

Since the onset of methicillin-resistant *S. aureus* strains (MRSA) in 1960 in the UK, *S. aureus* is in particular focus of science [106–108]. These infections are very expensive to treat and only a few effective antibiotics are available. The basis of this resistance is the gene *mecA*, which codes for a modified penicillin-binding protein (PBP2A). The β-lactam antibiotics can no longer bind to this protein and thus do not disrupt bacterial cell wall synthesis [109]. Often, MRSA strains show even more resistance to other classes of antibiotics and are therefore multi-drug resistant. Initially, MRSA strains were predominantly nosocomial, but in recent years they have been endemic in urban areas and are referred to as community-acquired MRSA (CA-MRSA). A special feature of CA-MRSA strains is their ability to resist methicillin, resulting in an improved virulence and fitness [110]. MRSA-related pneumonia is associated with the loss of tissue structure, hemorrhage, and consolidation of the

lung parenchyma [111]. The majority of MRSA infections is caused by the clone type USA300, which is of higher virulence than other MRSA strains, at least in animal models [112,113].

1.3 Co-infection with IAV and *S. aureus*

Pathogen evolution and the consequent development of influenza virus epidemics, but also pandemics can be explained by the necessity to evolve and adapt to new hosts and niches induced by environmental pressures. IAV pandemics are caused by the quick and high mutation rate of the vRNA genome, due to the lack of proof reading of polymerase activity. Because of the high nucleotide substitution, errors accumulate in newly synthesized RNA strands. Furthermore, IAV can undergo reassortment in mixed infections.

Common complications of respiratory diseases are caused by secondary bacterial infection. Synergistic lethality of influenza together with bacterial co-infection was initially observed in animal models shortly after influenza viruses were first isolated in early 1930s [114,115]. Lung tissue samples from the 1918 influenza pandemic suggest that the majority of the estimated 20–60 million deaths were caused by bacterial infections rather than from direct effects of the virus [2]. In seasonal epidemics, influenza virus and bacterial co-infection is associated with increases in hospital admissions [116,117], more severe symptoms [118], and increases in mortality [119].

Co-infection cases can be differentiated depending on the time of bacterial infection. *S. aureus* infection can occur three to ten days after viral infection, if the virus is still present in the organism, or only after successful elimination of the virus by the immune system [120]. Co-infection of IAV and *S. aureus* is often associated with the first group, while secondary pneumonia caused by *Streptococcus pneumoniae* (*S. pneumoniae*) usually belongs to the second group. Furthermore, the course of the disease in co-infection with IAV and *S. aureus* is described as progressing rapidly, with extensive pulmonary edema and hemorrhage. Despite adequate antibiotic treatment, lethal disease courses can often not be prevented [121–123]. Thus, detailed knowledge of the molecular events occurring through a co-infection, which are responsible for the aggravated disease process, is required.

1.3.1 Epidemiology

Perhaps the most prominent example of the devastating effect of bacterial pneumonia after IAV infection is the 1918 pandemic, also known as "Spanish flu". Retrospective analyses have shown that more than 95% of all deaths are due to bacterial pneumonia caused mainly by *S. aureus*, *S. pneumoniae*, *Haemophilus influenzae* and *Streptococcus pyogenes* (*S. pyogenes*) [2]. During the

following IAV pandemics in 1957 ("Asian Flu") and 1968 ("Hong Kong Flu"), only about 40% of all deaths were associated with bacterial co-infection. In 1957, *S. aureus*, in particular, was detected as a secondary pathogen, whereas in 1968, *S. pneumoniae* was predominant [124,125]. During the last 2009 pandemic ("swine flu"), bacterial pneumonia was detected in more than 25% of all serious or fatal cases, mostly caused by *S. aureus* or *S. pneumoniae* [126]. It was noticeable that especially in previously healthy patients an aberrant immune response occurred, which led to a fatal disease course [127].

The unpredictable nature of these outbreaks, in terms of their etiology and the reservoirs from which they arise, the constant emergence of new antigenic variants by mutation, combined with transmission within potentially immunologically naive populations facilitates the characteristic high proficiency of spread [128].

1.3.2 Co-pathogenesis

The mechanisms of co-pathogenesis between IAV and *S. aureus* are multifactorial. Both IAV and *S. aureus* express a variety of virulence factors, some of which are strain-dependent, that have a specific effect on the host in their respective combination. For example, the expression of the viral non-structural protein PB1-F2 or bacterial toxin PVL are responsible for increased inflammation after co-infection [112,129,130]. Concomitantly, numerous pathways of the host are affected. The most important mechanisms of co-pathogenesis between IAV and a bacterial pathogen are described in the following: Initially, influenza virus infect the upper respiratory tract. Virus replication occurs as described in 1.1.1, leading to cellular dysfunction, cell damage and death [131]. Influenza viruses with a poorly glycosylated haemagglutinin and the ability to engage both α2,3- and α2,6-linked sialic acids as receptors are able to penetrate deep into the lungs. The sialidase activity of the neuraminidase protein cleaves sialic acids from the surface of epithelial cells and from mucins that bind and eliminate virions, resulting in enhanced access to bacterial receptors [132]. These virus-mediated effects induce changes in the physical properties of the lungs and compromise innate immunity at several levels. Epithelial damage and increased receptor availability enable bacteria to adhere and grow. Depletion of the specific subset of lung macrophages that is functionally capable of phagocytosing bacteria enables escape from early innate immunity [133]. Furthermore, co-infection prevents effective regeneration and repair of the epithelium [134]. The infection spreads to the lower respiratory tract, which is clinically described as pneumonia. Usually, bacterial infection of the lower respiratory tract is barred by a combination of physical blockades and immune mechanisms [133]. The glottis prevents the gross aspiration of liquids and solids that might carry bacteria into the lungs [135].

Cilia sweep any debris or adventitious pathogens upwards and out of the bronchial tree and trachea, assisted by mucins and collagenous lectins that bind and neutralize pathogens [136]. Immune cells, complement and mucosal antibodies are activated upon recognition of pathogen invaders [137]. Respiratory viruses, such as influenza virus, disrupt host immune processes, which facilitates the emergence of bacteria from biofilms [138]. Further, influenza viruses can enable direct extension of the bacterial colonization via micro-aspiration into the lower respiratory tract. However, epidemiological evidence advocates that most invasive infections and pneumonia arise within a short period of time following the acquisition of a new bacterial strain. Systemic immunity (for example, pathogen-specific serum IgG) that is raised against colonizing bacteria confines the ability of these strains to successfully disseminate [139]. Thus, an alternative path to infect the lower respiratory tract might be by the direct inhalation of bacteria from the environment or a short-term colonization event in the upper respiratory. In this scenario, respiratory viruses contribute to the acquisition of pneumonia by increasing pathogen density in the nasopharynx and promote coughing and sneezing [140]. Subsequently, bacteria penetrate into the depths of the lungs in the person who is being afresh infected [141,142]. Ultimately, with the malfunction of various immune cells that can even lead to harmful behaviour ("friendly fire" pathology), large tissue lesions can appear as well as systematic invasion and sepsis can develop [143].

1.4 Inflammatory Response

Inflammation is a physiological response of the body to infections or other danger signals. It is a rapid, tightly regulated native immune response that elicits both local and systemic responses. The typical phenotype of acute inflammation consists of swelling, redness, pain, warming, and functional impairment [144]. These symptoms are mainly due to the release of soluble mediators such as the components of the complement system, eicosanoids, free radicals, cytokines and chemokines in the affected tissue, which on the one hand have a direct antipathogenic effect and on the other hand recruit other immune cells into the tissue. After elimination of the trigger, the tissue should return to homeostasis and there is a balance between pro- and anti-inflammatory signals [145]. Dysregulation of the inflammatory response results in serious consequences, as both acute and chronic severe tissue and organ lesions might occur, such as sepsis [146] and various autoimmune diseases [147].

1.4.1 Pro-Inflammatory cytokines and chemokines

Cytokines are peptides that have a fundamental role in communication within the immune system. They are expressed by several cell types, such as macrophages, T-cells, monocytes, leukocytes or

fibroblasts, and regulate inflammation [148]. Different cytokine families are structurally related but exhibit diverse functions (e.g., the TNF/TNF receptor, interleukin (IL)-1, IL-6 as well as interferon (IFN) superfamily). Furthermore, a classification based on the receptor specificity is also possible. The key cytokines of the pro-inflammatory response all bind to the type I cytokine receptors that in turn transmit signals to the recipient cell, leading to a change in function or phenotype [149]. Such signal cascades are complex and integrate a variety of environmental factors.

IFN, which is also part of the pro-inflammatory group, is divided into three groups, type I, II and III, depending on their amino acid sequence, evolution, structure and interaction with distinct receptor complexes. Up to now 13 IFNα genes, an IFNβ gene and other members such as IFNω, IFNε, IFNτ, IFNδ and IFNκ have been counted in type I IFNs [150]. In particular, IFNα and IFNβ exert antiviral function [151]. Moreover, IFN regulate the activation of immune cells, cell growth and apoptosis [152].

Pro-inflammatory chemokines are primarily produced by macrophages and neutrophils to recruit leukocytes to the sites of infection or injury [153,154]. They represent a group of small (8-14 kDa), basic and structurally related molecules with an important role in the host defence. In the last years, it became evident that chemokines exert an essential part in the development, homeostasis and function of the immune system [155]. To date, 44 chemokines and 23 chemokine receptors have been identified in the human genome [156]. The chemokine division system is mostly ruled by the position of the N-terminal cysteine residues. The C-X-C family presents a variable amino acid separating the first two cysteines, while the C-C family have them together.

During inflammation, there are some chemokines with an important role to maintain the body homeostasis. For instance, CXCL1 and CXCL2 are the first ones to be released, inducing neutrophil recruitment, and neutrophil active CCL3, CCL4 and CCL5 promote its entry into the site of tissue lesion. In addition, CCR4 and CCR5 stimulate activation of naive $CD8^+$ T-cells [157].

Chemokine signals are transduced through binding to members of the seven-transmembrane, G protein–coupled receptor (GPCR) superfamily [158], although there is also evidence that other effector pathways are possible [159]. The initial events in chemokine-induced signal transduction determine the outcome of the response and have to take place in the proximity of the receptor. These events include several tyrosine residue phosphorylations that direct the recruitment and activation of proteins that contain SH2 domains as mentioned before for the JAK-STAT pathway [160].

1.4.2 JAK-STAT pathway

Janus kinase (JAK)-signal transducer of activators of transcription (STAT) pathway is of crucial importance to transmit signalling obtained at the cell membrane to the nucleus and therefore key to the development and function of the immune system. JAK-STAT signalling is responsible for regulation of several cytokines, IFNs and growth factors, involved in critical cellular events, such as hematopoiesis and lactation [161–163]. JAKs are composed of seven JAK homology (JH) domains and possess a tandem architecture (JH1 and JH2 are distantly related to the other five domains) [164]. A catalytic domain and a kinase-like domain are essential, and, after ligand binding, receptor dimerization occurs. JAKs become activated by auto- or cross-phosphorylation and phosphorylate the cytoplasmic domain of the receptor, generating docking sites for recruitment of cytoplasmic adaptors that trigger the different mitogen-activated protein kinase (MAPK) pathways, extracellular signal-related kinase (ERK), JUN N-terminal kinase (JNK) and p38 (a class of MAPKs) or for signal transducer and activator of transcription factors known as STATs [165]. Phosphorylation plays a crucial role in the regulation of a multitude of signalling pathways [166]. Unphosphorylated STATs (Off) reside in the cytoplasm. In case of JAK-mediated STAT phosphorylation (On), STATs dimerize [167] and migrate to the nucleus where they bind to specific DNA sequences in the promoters of target genes to activate or repress them [168]. Thus, the JAK-STAT cascade provides a direct mechanism to translate an extracellular signal into a transcriptional response.

1.4.2.1 STAT1

STAT1 is a complex protein with several but contrasting functions that upon activation, leads to the expression of many genes but also to the suppression of others [169]. It presents two isoforms: the longer STAT1α (91 kDa) and the shorter STAT1β (84 kDa) [170,171]. Spliced from STAT1, STAT1β comprises a truncated version of STAT1. This molecule lacks 38 amino acids due to the deletion of the last 118 nucleotides. Thus, compared to STAT1α, STAT1β lacks most of the transactivation domain as well as a serine 727 phosphorylation site in the C-terminus [172,173]. Although not lethal at birth, selective gene deletion of STAT1 in mice leads to rapid death from severe infections [174,175], demonstrating its major role in the response to pathogens. Similarly, in humans who do not express STAT1, there is a lack of resistance to pathogens leading to premature death [176,177]. This indicates a key, non-redundant function of STAT1 in the defence against pathogens. As mentioned before, STAT1 is an essential effector of IFNs. And following interaction of IFNα/β with the two subunits of its receptor [178,179], JAK1 and TYK2 phosphorylate one another [180] and subsequently phosphorylate both interferon-α/β receptor (IFNAR)1 and IFNAR2 [181]. This process will then support STAT1 binding sites establishment [182]. STAT1 binds via its Src homology 2 (SH2) domain to STAT2 [183] and is

phosphorylated on tyrosine 701 [184,185]. The phosphorylated STAT1/STAT2 dimer is then released from the IFNAR2 chain. Subsequently, the dimer association with the DNA-binding Interferon regulatory factor 9 (IRF9) results in the formation of the IFN stimulated gene factor 3 (ISGF3) complex, which translocates to the nucleus by binding to importin-α5. In the nucleus, the complex binds to the promoters of IFN stimulated genes (ISGs) by recognizing the interferon-stimulated response element (ISRE) and activates gene expression (Fig. 4) [186,187].

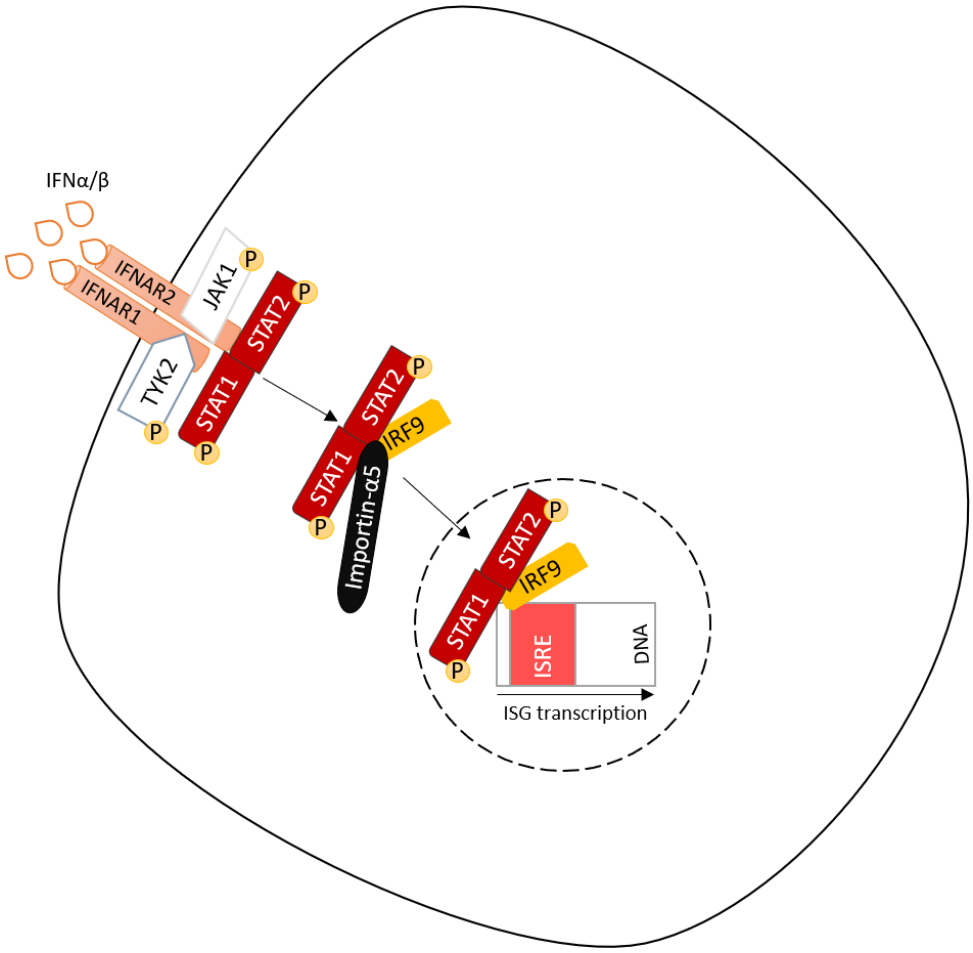

Fig. 4. Scheme of type I IFN-dependent signalling and ISGF3-mediated gene expression. After type I IFN binding to its receptors, which are pre-associated to the kinases TYK2 and JAK1, a trans-phosphorylation of these kinases occurs by close proximity. This will lead to phosphorylation of IFNAR intracellular chains that will provide docking sites for STAT1 and STAT2. Both will be phosphorylated, resulting in dimerization and association with IRF9, forming a complex called ISGF3 that needs the help of importin-α5 to translocate to the nucleus. Finally, ISGF3 recognizes ISRE and induces the expression of ISGs, which are essential to the cell defence against pathogens.

1.4.3 Immune response after IAV infection

Infection with IAV leads to the stimulation of the innate immune system and the expression of pro-inflammatory cytokines and chemokines. An antiviral effect is achieved primarily by the induction

of type I IFN, which efficiently combats viral replication and virus spread. At the same time, IAVs have developed numerous mechanisms that counteract the antiviral immune response, e.g. IAV expresses the viral protein NS1, which inhibits type I IFN induction as well as the effect of the type I IFN reply [35,36]. Type I IFN induction is inhibited by competing of NS1 with cellular proteins for double stranded RNA binding sites [188], by binding to a factor responsible for transcriptional ending and polyadenylation (CPSF) as well as interfering with nuclear exportation of cellular mRNA [189]. Similarly, the viral protein PB1-F2 inhibits IFN induction by interacting with the mitochondrial antiviral signalling protein (MAVS), which leads to a blockage of the Interferon-regulatory factor 3 (IRF3) signalling pathway [190,191]. For the subunits of the viral polymerase PB1, PB2 and PA as well as for NP also IFN-antagonistic abilities were shown [38,192,193]. Additionally, other proinflammatory cytokines and chemokines are released, which activate the chemotaxis of immune cells such as macrophages and neutrophils and initiate the adaptive immune system. Increased levels of TNFα, IL-1β, IL-6, IFNγ, CCL2, CCL3 and CXCL10 are also observed in some situations, after IAV infection, which is described as "cytokine storm" [194–196] that could lead to life-threatening immunopathology with tissue lesions [197].

1.4.4 Immune response after S. aureus infection

S. aureus is a commensal bacterium constantly colonizing the body in its exposed epithelial surfaces, e.g., on skin and mucosa on about 30% of the population [102]. It is able to induce a pro- but also an anti-inflammatory response. Toll-like-receptor (TLR)-2 is responsible for the local production of soluble mediators, such as cytokines, chemokines and antimicrobial peptides as a result of the first interaction of the bacteria with epithelial cells [198–200]. TLR-2 then triggers an immune stimulatory effect on epithelial cells and a broad range of immune cells, but it is not solely responsible for bacterial clearance or containment of adherent *S. aureus* on the epithelial surfaces [201]. The type I IFN response is also activated after *S. aureus* infection, resulting in the production of IFNβ and enhanced IFN-stimulated gene (ISG) expression [202]. However, *in vivo* models show that the IFN response has more of a harmful than protective effect, as IFNAR $^{-/-}$ mice have a reduced mortality after *S. aureus* infection [203]. Systemic inflammation after *S. aureus* infection leads to sepsis, with increased amounts among others of TNFα, IL-6, IL-12 and IFNγ, so that cytokine-induced inflammation is more harmful than primary infection [204,205].

1.5 Objective

Given the clear health threat presented by influenza viruses and *S. aureus*, which is even more serious when they “team up” against our immune system, it is then of major importance to study

the regulatory molecular mechanisms. The immunopathology associated to the co-infection persists even with the use of sterilizing antibiotics [206] and the depletion of T-lymphocytes, macrophages or neutrophils has no influence on the course of co-infection [112], suggesting a role of other cell types, like epithelial cells.

And even though recent work started to unravel cellular signalling pathways that are deregulated in presence of IAV and *S. aureus* [207], nothing is known about specific pathogen components responsible in the devastating pathogen-host interaction. In case of the *S. aureus*-mediated inhibition of IAV-induced type IFN response, the bacterial factor responsible is unknown [207]. Warnking and her colleagues achieved several findings which turned out to be the basis for this project. As a result of a combined infection with IAV and *S. aureus* 6850, reduced ISG expression as well as an increase in the virus replication was shown [207]. The results pointed to a block of STAT1-STAT2 dimerization in presence of *S. aureus*. While phosphorylation of JAK1 and STAT2 still occurs, a reduced STAT1 phosphorylation state in a co-infection scenario that blocks STAT1-STAT2 dimerization and impairs the antiviral response was shown [207]

The present work aimed to characterize the factor responsible for the diminished STAT1 phosphorylation state by applying mutants of interest with essential known roles in bacterial pathogenicity and persistence to a co-infection scenario [95]. Using SH1000, a laboratory strain, and LS1, an isolate like 6850, it was also important to verify if this inhibition was a strain specific event and the differences between them.

Further, the induction of the pro-inflammatory response in human alveolar epithelial cell lines after co-infection with both wild-type pathogens (and mutants of interest) *in vitro* or co-stimulation with IFNβ was monitored.

2. Material

2.1 Used Devices

BioPhotometer	Eppendorf (Hamburg)
Blot chamber	BioRad (Munich)
Blood agar plates	Oxoid (Basingstoke, UK)
Cell scrapers	Sarstedt (Nümbrecht)
Centrifuge 5417R and 5810R (coolable)	Eppendorf (Hamburg)
Counting chamber (Neubauer)	Merck (Darmstadt)
Cuvettes	Sarstedt (Nümbrecht)
Dishes for cell culture (15 cm)	Greiner Bio-One (Frickenhausen)
Falcon Tubes (15 mL; 50 mL)	Greiner Bio-One (Frickenhausen)
Flasks for cell culture (T25; T75; T175)	Greiner Bio-One (Frickenhausen)
HeraCell 24G (CO_2-Incubator for cell culture)	Heraeus (Hanau)
Inoculation loops	Sarstedt (Nümbrecht)
Intelli Mixer RM2 (Overhead shaker)	Elmi (Riga, Latvia)
Multiwell plates for cell culture (6-well; 12-well)	Greiner Bio-One (Frickenhausen)
NanoDrop NP-1000	PEQLAB Biotechnologie (Erlangen)
New Brunswick Galaxy 48R (CO_2-Incubator for co-infection)	Eppendorf (Hamburg)
Odyssey Fc Imaging System	LI-COR (Bad Homburg)
pH-Meter 765 Calimatic	Knick (Berlin)
Pipettes (2 mL; 5 mL; 10 mL; 25 mL)	Greiner Bio-One (Frickenhausen)
Pipette's tips (10 µL; 200 µL; 1000 µL)	Sarstedt (Nümbrecht)
Plastic tubes (10 mL)	Sarstedt (Nümbrecht)
Power Supply Power Pac Basic 300	BioRad (Munich)
PROTRAN Nitrocellulose Transfer Membrane	GE Health Care Life Sciences (Freiburg)
Reaction vessels (1.5 mL; 2 mL)	Eppendorf (Hamburg)
Shaker Duomax 1030	Heidolph (Schwabach)
Sirius Medicalsafe Slimline Scanlaf (Sterile bench for co-infection)	Labogene (Lynge, Denmark)
Sterile bench for cell culture	BDK (Sonnenbühl-Genkingen)
Thermomixer comfort	Eppendorf (Hamburg)
Vortex-Genie 2	Scientific Industries (Bohemia, USA)
Whatman GB002 paper	Schleicher & Schüll (Dassel)

2.2 Chemicals

Acrylamide/Bisacrylamide (37.5:1)	Serva (Heidelberg)
Albumin Fraction V	Roth (Karlsruhe)
Ammonium persulfate (APS)	Roth (Karlsruhe)
Aprotinin	Roth (Karlsruhe)
Benzamidine	Sigma-Aldrich (Munich)
β-mercaptoethanol	Roth (Karlsruhe)
BioRad protein assay dye reagent	BioRad (Munich)
Bromophenol blue	Sigma-Aldrich (Munich)

Calcium chloride ($CaCl_2$)	Roth (Karlsruhe)
DEAE-Dextran	Sigma-Aldrich (Munich)
Ethanol	Roth (Karlsruhe)
Ethylenediaminetetraacetic acid (EDTA)	Sigma-Aldrich (Munich)
Gentamicin	Sigma-Aldrich (Munich)
Glycerol	Roth (Karlsruhe)
Glycerol-2-phosphate	Sigma-Aldrich (Munich)
Glycin	Roth (Karlsruhe)
Leupeptin	Serva (Heidelberg)
Lysostaphin	Sigma-Aldrich (Munich)
Magnesium chloride ($MgCl_2$)	Roth (Karlsruhe)
Methanol	Roth (Karlsruhe)
Milk powder	Roth (Karlsruhe)
Neutral red	Sigma-Aldrich (Munich)
Oxoid-Agar	Oxoid (Basingstoke, UK)
PageRuler^{TM} prestained protein ladder	Fermentas (St. Leon-Rot)
p-coumaric acid	Roth (Karlsruhe)
Pefablock	Roth (Karlsruhe)
Phosphate buffered saline (PBS)	Sigma-Aldrich (Munich)
Protein G agarose beads	Sigma-Aldrich (Munich)
Sodium acetate ($C_2H_3NaO_2$)	Applichem (Darmstadt)
Sodium chloride (NaCl)	Roth (Karlsruhe)
Sodium dodecyl sulfate (SDS)	Roth (Karlsruhe)
Sodium pyrophosphate	Sigma-Aldrich (Munich)
Sodium orthovanadate	Sigma-Aldrich (Munich)
Tris(hydroxymethyl)aminomethane	Roth (Karlsruhe)

2.3 Cell culture material

10x MEM	Gibco Invitrogen (Karlsruhe)
100x Penicillin/Streptomycin	Gibco Invitrogen (Karlsruhe)
Brain-Heart infusion medium (BHI)	Merck (Darmstadt)
Bovines serum albumin (35%; BSA)	MP Biomedicals (Eschwege)
Dulbecco's modified eagle medium (DMEM; with 4.5 g l^{-1} Glucose, L-glutamine, $NaHCO_3$, Pyridoxine, HCL)	Sigma-Aldrich (Munich)
Fetal calf serum (FCS)	Biochrom (Berlin)
HEPES	Gibco Invitrogen (Karlsruhe)
Minimum essential medium (MEM; with Earle's salts, L-glutamine, $NaHCO_3$)	Sigma-Aldrich (Munich)
Sodium hydrogencarbonate (7.5%; $NaHCO_3$)	Gibco Invitrogen (Karlsruhe)
Trypsin-EDTA	Gibco Invitrogen (Karlsruhe)
TPCK-Trypsin	Sigma-Aldrich (Munich)

2.4 RNA work material

RNeasy kit	Qiagen (Hilden)
5x reaction buffer for H minus reverse transcriptase (RT)	Fermentas (St. Leon-Rot)

2x Brilliant® III SYBR Green®	Agilent Technologies (Waldbronn)
dNTPs	Sigma-Aldrich (Munich)
Oligo-(dT)-Primer	Eurofins MWG Operon (Ebersberg)
Random Hexamer Primer	Fermentas (St. Leon-Rot)
Revert Aid™ H minus RT	Fermentas (St. Leon-Rot)

2.4.1 Primers for human probes

*aroE*_fwd	5' CTATCCACTTGCCATCTTTTAT 3' [208]
*aroE*_rev	5' ATGGCTTTAATATCACAATTCC 3' [208]
*GAPDH*_fwd	5' GCAAATTCCATGGCACCGT 3' [207]
*GAPDH*_rev	5' GCCCCACTTGATTTTGGAGG 3' [207]
*IFNβ*_fwd	5' TCTGGCACAACAGGTAGTAGGC 3' [209]
*IFNβ*_rev	5' GAGAAGCACAACAGGAGAGCAA 3' [209]
*M1*_fwd	5' AGATGAGTCTTCTAACCGAGGTCG 3' [210]
*M1*_rev	5' TGCAAAAACATCTTCAAGTCTCTG 3' [210]
*MxA*_fwd	5´ GAAGGGCAACTCCTGACAGT 3´ [207]
*MxA*_rev	5´ GTTTCCGAAGTGGACATCGCA 3´ [207]
*TRAIL*_fwd	5' GTCTCTCTGTGTGGCTGTAACTTACG 3' [207]
*TRAIL*_rev	5' AAACAAGCAATGCCACTTTTGG 3' [207]

2.5 Cell lines

Name	Description	Culture medium
A549	Human alveolar basal epithelial cells	DMEM, 10% FCS
Madin-Darby canine kidney (MDCK)	Dog renal epithelial cells	MEM, 10% FCS

2.6 Pathogens

2.6.1 IAV strains

Name	Origin
A/Puerto Rico/8/34 (H1N1) (PR8-M)	[192]

2.6.2 S. aureus strains

Name	Description	Origin
6850	Isolate from an osteomyelitis patient	GenBank ATCC536657
SH1000	Laboratory strain, NCTC8325-4 derivative	[211]
SH1000 ΔsigB	SH1000 derivative carrying the *rsbUVWsigB* deletion of IK181; Em^R	[95]
SH1000 Δagr	SH1000 derivative carrying the *agr*::*tet* mutation of RN6911; Tc^R	[212]
SH1000 ΔsarA	SH1000 derivative carrying the *sarA*::Km mutation of PC1839; Km^R	[212]

SH1000 Δagr + ΔsarA	SH1000 derivative carrying the *agr*::*tetM* and *sarA*::Km mutations of RN6911 and PC1839, respectively; Tc^R, Km^R	A. Cheung, unpublished
LS1	Murine isolate from a septic arthritis patient	[83]
LS1 ΔsigB	LS1 derivative carrying the *rsbUVWsigB* deletion of IK181; Em^R	[213]
LS1 Δagr	LS1 derivative carrying the *agr*::*tetM* deletion of RN6911; Tc^R	[95]
LS1 ΔsarA	LS1 derivative carrying the *sar*::Tn*917*LTV1 mutation of ALC136; Em^R	[95]
LS1 Δagr + ΔsarA	LS1 derivative carrying the *agr*::*tetM* and *sar*::Tn*917*LTV1 mutations of RN6911 and ALC136, respectively; Em^R, Tc^R	[95]

2.7 Media and buffers

Blot buffer

192 mM Glycin

25 mM Tris

15% (v/v) Methanol

BHI medium

37 g in 1 L ddH_2O

Enhanced chemiluminescence (ECL)

2.5 mM Luminol

0.36 mM p-coumaric acid

100 mM Tris/HCl pH 8.5

0.015% (v/v) H_2O_2

Infection medium

0.21% (w/v) BSA

0.01% (w/v) Ca^{2+}/Mg^{2+}

3 ng mL^{-1} TPCK-Trypsin

in medium

Infection PBS

1 mM $MgCl_2$

0.9 mM $CaCl_2$

100 U mL^{-1} Penicillin

0.1 mg mL^{-1} Streptomycin

0.2% BSA

in PBS

Invasion medium

0.2% (v/v) HSA

1 mM HEPES

in Medium

MEM (1.5×)

1.5% (v/v) 10× MEM

0.3% (v/v) $NaHCO_3$

0.015% (w/v) DEAE-Dextran

0.35% (w/v) BSA

Plaque medium

70 % (v/v) 1.5× MEM

0.9 % (w/v) Oxoid-Agar

0.01 % (w/v) Ca^{2+}/Mg^{2+}

4 ng mL^{-1} TPCK-Trypsin

SDS-PAGE separating buffer (5×)

25 mM Tris/HCl pH 8.5

250 mM Glycin

0.1% (w/v) SDS

SDS-PAGE sample buffer (5×)

10% (w/v) SDS

50% (v/v) Glycerol

25% (v/v) β-Mercaptoethanol

0.1% (v/v) Bromophenol blue

312 mM Tris/HCl pH 6.8

SDS-PAGE stacking gel

178 mM Tris/HCl pH 6.8

1% (v/v) TEMED

0.1% (w/v) SDS

0.1% (w/v) APS

1% (v/v) Acrylamide/Bisacrylamide (37.5:1)

SDS-PAGE running gel

370 mM Tris/HCl pH 8.9

0.02% (v/v) TEMED

0.1% (w/v) SDS

0.1% (w/v) APS

7.5% (v/v) Acrylamide/Bisacrylamide (37.5:1)

Stop medium

10% (v/v) FBS

0.1 mg mL^{-1} Gentamicin

in medium

TBS-Triton wash buffer (TBS-T)

50 mM Tris/HCl pH 7.6

150 mM NaCl

0.2% (v/v) Triton-X100

TLB lysis buffer pH 8.3

20 mM Tris/HCl pH 7.4

137 mM NaCl

10% (v/v) Glycerol

1% (v/v) Triton-X100

2 mM EDTA pH 8.0

50 mM Glycerol-2-phosphate

20 mM Na-Pyrophosphate

Add fresh:

1 mM Sodium orthovanadate

5 mM Benzamidine

0.2 mM Pefablock

5 µg mL^{-1} Leupeptin

5 µg mL^{-1} Aprotinin

Western Blot blocking solution

5% (w/v) Milk Powder in TBS-T

2.8 Antibodies

Anti-p44/42 MAPK (ERK1/2) rabbit #9102 | p44 MAP Kinase C-terminus | Cell Signalling Technology

Anti-PB1 (D-8) mouse monoclonal IgG3 κ | human PB1 aa. 33-71 C-terminus | Santa Cruz Biotechnology

Anti-Peptidoglycan 3F6B3 (10H6) mouse monoclonal IgG_1 | 3D polymer complex structure of peptidoglycan (PG) | Bio-Rad Laboratories

Anti-Phospho-Stat1 (Tyr701) (58D6) rabbit mAb #9167 | human Stat1 - Tyr701 | Cell Signalling Technology

Anti-Phospho-Stat2 (Tyr689) rabbit polyclonal IgG | mouse Stat2 – Tyr689 | Merck (Upstate)

Anti-Stat1 mouse monoclonal IgG_1 | human Stat1 aa. 1-194 N-terminus| BD Transduction Laboratories™

Anti-Stat2 (A-7) mouse monoclonal IgG_1 | human Stat2 aa. 832-851 C-terminus | Santa Cruz Biotechnology

Anti-Stat2 (B-3) mouse monoclonal IgG_1 | human Stat2 aa. 7-26 N-terminus | Santa Cruz Biotechnology

IRDye® 800CW donkey anti-mouse IgG (H + L), 0.5 mg | LI-COR

IRDye® 800CW donkey anti-rabbit IgG (H + L), 0.5 mg | LI-COR

IRDye® 680RD donkey anti-rabbit IgG (H + L), 0.5 mg | LI-COR

IRDye® 680RD donkey anti-mouse IgG (H + L), 0.5 mg | LI-COR

3. Methods

3.1 Cell Culture Techniques

All work was performed under sterile conditions and with endotoxin-free materials at a level II sterile workbench. The cultivation of the cells was carried out in incubators with a saturated atmosphere at 37°C and 5% CO_2 content.

3.2 Virological Methods

The IAV used is a human isolate of risk group 2 and was accordingly handled in laboratories of safety level 2 and stored there at -80°C.

3.2.1 *Virus Growth*

For the propagation of A/Puerto Rico/8/34 (H1N1) (PR8-M), MDCK II cells were used. Infection of the cells was performed at a degree of confluence of about 80% by adding the virus with a multiplicity of infection (MOI) of 0.001 to the infection medium. After 48-72 h, a significant cytopathic effect became visible, cell supernatants were collected, and cell debris was removed by centrifugation for 20 min at 3220 rcf (4000 rpm), 4°C.

3.2.2 *Determination of infectious virus particles - plaque assay*

The detection of infectious virus particles was achieved indirectly via the detection of plaques, which became visible as holes in the confluent cell layer. For this purpose, MDCK II cells were seeded in 6-well plates, so that the next day a confluent cell layer was present. The virus was serially diluted in infectious PBS. The cells were washed with PBS and then infected with 500 µL of the diluted virus suspension. After 0.5 h incubation at 37°C, the supernatant was aspirated and 2 mL of plaque medium was added to the cells. The agar contained in the medium prevented the diffusion of the virus particles. In consequence, adjacent cells were infected by newly synthesized viruses. It can be assumed that each infectious virus particle produced a plaque in the cell layer. After 48 to 72 h, the cells were stained with neutral red and the plaques were counted. The determination of the virus titre (plaque-forming units, PFU) was done with the following formula:

Number of plaques × dilution level × 2 = PFU mL^{-1}

3.3 Bacteriological Methods

S. aureus was cultivated on blood agar plates at 4°C. Every four weeks, these plates were changed and fresh blood agar plates were inoculated with bacteria stored in glycerol at -80 °C.

3.3.1 Cultivation, preservation and inactivation of prokaryotic cells

For each *in vitro* experiment, a fresh overnight culture (ONC) was performed the night before. For this purpose, 5 mL of BHI medium plastic tube was inoculated with a colony from a blood agar plate in a plastic tube and incubated at 37°C. Before the start of the experiment, the cells were pelleted by centrifugation for 5 min at 3220 rcf (4000 rpm), 4°C, washed once in 5 mL PBS and resuspended in PBS. The number of bacteria was measured by determining the optical density (OD) at 600 nm. By growth kinetics it was determined that at $OD_{600} = 1$, a concentration of $5x10^8$ colony forming units (CFU) mL^{-1} is present.

3.3.2 Determination of bacterial titres

To quantify live bacteria, the supernatants were serially diluted in PBS. Subsequently, 50 µL of bacterial suspension was applied onto BHI agar plates. After overnight incubation at 37°C, colonies were counted and the bacterial titres were calculated using the formula:

Number of colonies x dilution level x 20 = CFU mL^{-1}

For the determination of intracellular bacteria after *in vitro* infection, the cells were washed 0.5 h before the end of incubation with PBS and incubated with 2 µg mL^{-1} lysostaphin in infection medium to lyse extracellular bacteria. The cells were washed twice with PBS and incubated for 0.5 h with 2 mL ddH_2O at 37°C to lyse the cells by osmotic shock. The lysate was transferred to a plastic tube, pelleted for 15 min at 3220 rcf (4000 rpm), 4°C and resuspended in 1 mL PBS. A serial dilution with PBS was then performed and a 40 µL inoculation on BHI agar plates was made. After overnight incubation at 37°C, colonies were counted.

3.4 Co-infection Model

3.4.1 Co-infection in vitro

A549 cells were grown in 6-well plates ($0.5x10^6$) in 2 mL of culture medium or in 12-well plates ($0.25x10^6$) were seeded in 1 mL of culture medium for 16 h before the start of the experiment.

The cells were washed with PBS and incubated with 5 MOI IAV in 500µL of infectious PBS for 0.5 h at 37°C. The supernatant was aspirated. The cells were washed with PBS and incubated for 3 h at 37°C with 1 mL invasion medium containing MOI 50 *S. aureus*. The medium was aspirated, cells were washed with PBS and incubated with 1 mL of stop medium for 0.5 h at 37°C. The stop medium contained the antibiotic gentamicin (0.1 mg mL^{-1}) to kill extracellular bacteria, which did not internalize so far.

Subsequently, the medium was removed, the cells were washed with PBS and incubated in 1 mL of infection medium until the end of the incubation period.

To improve the infection efficiency, 5 MOI IAV in 300µL of infectious PBS and 50 MOI *S. aureus* in 500 µL invasion medium was used.

3.5 Stimulation of eukaryotic cells

To exclude interfering side effects of replicating IAV on IFN-mediated signal transduction processes, recombinant IFNβ was used as a stimulus. A549 cells were infected with *S. aureus* 6850 and SH1000 strains (MOI 50) as described above. Extracellular bacteria were removed 3 h after bacterial infection by treatment with gentamicin (0.1 mg mL^{-1}) for 0.5 h. Subsequently, the cells were washed and, after an incubation period of 7.5 h, 500 U recombinant human IFNβ solved in infection medium was added for 30 min.

3.6 Protein work

3.6.1 Production of protein extracts

For the extraction of proteins from *in vitro* experiments, the cells were washed twice with PBS and lysed directly in 1 × sodium dodecyl sulfate (SDS)-PAGE sample buffer, to ensure efficient bacterial lysis. Thus, bacterial proteins could be detected in the lysates. After incubation overnight at 4°C on a shaker, the samples were transferred to reaction vessels and denatured at 95°C for 7 min.

3.6.2 SDS polyacrylamide gel electrophoresis (SDS-Page)

The SDS-Page allows the separation of denatured proteins according to their size. For this purpose, a discontinuous gel was used, containing a lower acrylamide concentration in the collecting gel and a higher acrylamide concentration in the separating gel.

The crosslinking of the acrylamide monomers forms a three-dimensional gel matrix with different pore size, depending on the acrylamide concentration. In the collecting gel,

containing larger pores, the proteins were concentrated, before being separated in size in the separating gel, characterized by smaller pores. The pH change from the collecting to the separating gel led to a further focus of the protein bands. To achieve a uniform migration in the electric field from cathode to anode, protein charge was masked by SDS negative charge, which was also present in the SDS-Page separating buffer. The run was performed at a constant voltage of 20 mA. The size of the proteins was determined by comparison with a parallel running PageRuler^{TM} prestained protein ladder.

3.6.3 Western Blot

The separated proteins in the gel were transferred to a nitrocellulose membrane and immobilized thereon by means of hydrophobic interactions and hydrogen bonds. The process of wet blotting was used and a continuous current of 400 mA was applied for 55 min. The membranes were incubated for 1 h in Western Blot blocking solution to saturate free binding sites on the membrane and washed with TBS-T for 0.5 h. The proteins were detected with specific primary antibodies, which were incubated in TBS-T with 5% albumin overnight at 4°C shaking. The following day, the membrane was washed with TBS-T for 10 min and incubated for 1 h with secondary antibodies in TBS-T. Finally, the membrane was washed for 3x 10 min in TBS-T and electrochemiluminescence (ECL) solution was applied for 1 min. To activate the ECL, 6.1 µL of H_2O_2 was added to the solution. Lastly, the membrane was inserted in an appropriate sleeve to be analysed in the LI-COR machine (Odyssey).

3.6.4 Co-Immunoprecipitation (Co-IP)

A Co-IP allows the detection of a specific protein-protein interaction. Here an antibody is coupled to a stationary phase, the agarose beads. This complex is able to specifically interact with specific proteins connected to other proteins, which can be detected by respective antibodies upon denaturation and separation on a SDS-PAGE. The cells were lysed in 200 µL of TLB buffer for 0.5 h at 4°C on a shaker. The samples were inserted in a reaction vessel, centrifuged for 10 min at 20817 rcf (14000 rpm), 4°C and the amount of protein was determined by means of Bradford determination [214]. 5 µL lysate was mixed with 995µL BioRad protein assay dye solution (diluted 1:5 in ddH_2O) in a cuvette. The contained coomassie blue forms a complex with the proteins, this leads to a shift of the absorption maximum, so that determination of the protein concentration was carried out photometrically at 595 nm. The protein content was adjusted with TLB buffer in all samples.

Lastly, 0.5 mL lysate was mixed with 30µL protein G agarose beads and 10 µL STAT2 antibody for IP samples. Input controls got adjusted but didn't receive the agarose beads and STAT2 antibody treatment. The IP samples were incubated overnight at 4°C on an overhead shaker. Finally, the IP samples were washed twice with TLB buffer for 2 min at 500 g, 4°C. The precipitated antigen antibody complexes were spiked with 30 µL 2× SDS-PAGE sample buffer containing β-mercaptoethanol and denatured for 1.5 min at 95°C. Separation and detection of proteins was achieved by SDS-Page and Western Blot (See above; IP samples need centrifugation before loading the gel to avoid loading the beads).

3.7 RNA work

For RNA work, only RNase-free materials and reagents were used.

3.7.1 RNA isolation using RNeasy Kit (Qiagen)

For the isolation of RNA from *in vitro* experiments, the RNeasy kit from Qiagen was used. This contained silica gel membrane columns that selectively bound RNA of at least 200 nucleotides in size. The purification was performed according to the manufacturer protocol:

The cells were washed twice with PBS and treated with lysis buffer containing denaturing guanidine isothiocyanate and 1% β-mercaptoethanol to inhibit RNases. After homogenization, the lysate was mixed with 200 µL 70% ethanol and added to the columns. Upon several washes, the RNA was eluted in 30 µL of DEPC-H_2O, the concentration and purity were determined by NanoDrop™ measurement and samples were stored at -80°C until further use.

3.7.2 Reverse transcription of RNA (cDNA synthesis)

To determine the mRNA levels of various cytokines and chemokines after infection and stimulation, the isolated RNA was rewritten with oligo (dT) primers, which bind complementarily to the poly(A)-tail of the mRNA, and a reverse transcriptase into cDNA. However, since bacteria don't present poly(A)-tail, for bacterial samples and for bacterial control determination, random hexamer primers in detriment of oligo (dT) primers were used to obtain more accurate values. For this purpose, equal amounts of RNA were mixed in 11 µL DEPC-H_2O with 0.5µg each Oligo-(dT)/random hexamer and denatured for 10 min at 70°C. After cooling on ice, each sample was added to the reaction mixture (4 µL 5x reaction buffer, 2 µL 10 mM dNTPs, 0,5 µL 200 U mL^{-1} Revert Aid™ H minus RT and 1,5 µL

DEPC-H_2O). The samples were incubated for 10 min at 37°C to allow attachment of the primers to the RNA. Then, the transcription into cDNA was carried out for 1 h at 42°C and was finally stopped with a 10 min incubation step at 70°C. The cDNA was stored at -20°C until use.

3.7.3 Quantitative Real-Time PCR (qRT-PCR)

During a qRT-PCR, a specific product is amplified, and the amount of this product is detected in parallel. This is achieved by using a fluorescent dye (Brilliant® III SYBR Green®), which is non-specifically intercalated with double-stranded DNA. Thus, the fluorescence intensity is proportional to the amplified amount of the PCR product and quantification is possible.

The previously synthesized cDNA was diluted in DEPC-H_2O (0.5 µL cDNA, 6.7 µL DEPC-H_2O) and each sample was analysed in duplicates. For the PCR reaction, the following approach per sample was chosen:

4 µL 2× Brilliant® III SYBR Green®; 0.6 µL 10 µM primer mix (fwd + rev in DEPC-H_2O), and 0.2 µL Reference Dye.

Program:

1. Initial denaturation ---------- 95°C ---------- 3 min
2. Denaturation, Annealing ---------- 95°C ---------- 5 s
   Elongation (50 cycles) ---------- 60°C ---------- 10 s
3. Melting curve ---------- 95°C ---------- 1 min
4. Cooling

The melting curve indicated the specificity of the elapsed reaction. To normalize the values, the mRNA levels of glyceraldehyde-3-phosphate dehydrogenase (GAPDH) were used as it is expressed almost independently of the cell cycle or experimental treatment. The evaluation of the qRT-PCR was carried out according to the $2^{-\Delta\Delta Ct}$ method [215].

4. Results

The secondary bacterial pneumonia, often caused by *S. aureus* is one of the most dangerous threats upon IAV infections. After the 1918 pandemic, where almost 95% of deaths were related bacterial secondary infections [2], the extreme importance to study and to uncover the molecular regulatory mechanisms became obvious.

4.1 The type I IFN-mediated signalling is blocked in presence of *S. aureus* infection

It has been recently shown that *S. aureus* is able to inhibit the type I IFN-mediated signalling resulting in the down-regulation of IFN-stimulated genes (ISGs) [207]. To understand the molecular mechanism behind, a co-infection model was optimized. The human alveolar basal epithelial cell line A549 representative of the lower respiratory tract were sequentially infected with IAV and *S. aureus* allowing the study of this particular impaired step in the JAK-STAT pathway.

Thus, A549 cells were infected with A/Puerto Rico/8/34 (H1N1) (PR8M) for 0.5h and subsequently *S. aureus* 6850 were added. At 3.5h post-infection (p.i.) with IAV and 3h p.i. with *S. aureus*, respectively, extracellular bacteria were removed by gentamicin treatment and the cells were further incubated until the end of the first viral replication cycle (8h p.i.). Afterwards, phosphorylation of STAT1 and the virus titres were analysed (Fig. 5). The data indicate the reduction of STAT1 phosphorylation (Fig. 5A) and a slight increase of virus titres in presence of bacteria (Fig. 5B, C) correlating to the effects that Warnking and her colleagues already demonstrated [207].

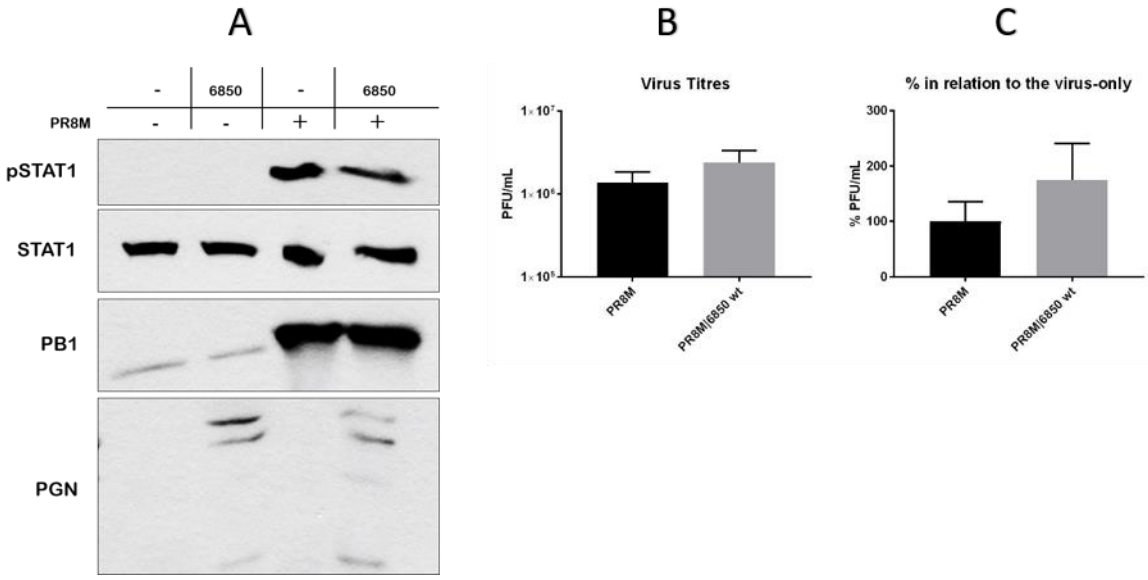

Fig. 5. Influenza virus-induced STAT1 phosphorylation is reduced upon *S. aureus* 6850 co-infection (A) associated with increased virus titres (B, C). A549 cells received a mock treatment or were infected with the influenza virus A/Puerto Rico/8/34 (PR8M) H1N1 (MOI = 5) for 8h. Co-infection with *S. aureus* 6850 wild-type (wt) (MOI = 50) was performed 30 min post-infection (p.i.). Extracellular bacteria growth was stopped by a gentamicin treatment and a PBS wash step 3 h post bacterial infection. Whole cell lysates were subjected to WB analysis monitoring phosphorylated STAT1 (Y701) (pSTAT1), the viral polymerase protein (PB1) and the bacterial protein (PGN). Detection of STAT1 served as loading control (A). Western Blot (WB) analysis is representative of at least three independent experiments. Progeny virus titres were determined by standard plaque assay and shown as PFU ml^{-1} (B) and n-fold of PR8M-only infected control (C). Data represent the means ± SD of at least three independent experiments. Statistical significance was evaluated by a one-way ANOVA followed by Dunnett's multiple comparison test (*P < 0.05).

Based on this work, other *S. aureus* strains (e.g. SH1000, LS1) and different bacterial mutant strains should be investigated within the present work to unravel the bacterial factors responsible for this phenomenon.

Initially, the SH1000 strain and different mutants were used in the co-infection model mentioned above. Co-infection of A549 cells with PR8M and *S. aureus* SH1000 wild-type (wt) and the mutant strains resulted in a reduction of the IAV-induced STAT1 phosphorylation. Most obvious the reduction was visible upon infection with the *S. aureus* double mutant strain (*agr* and *sarA*), which as a result of genetic manipulation, doesn´t possess two important virulence players of *S. aureus* (Fig. 6A). It is reported that concomitant silencing of *agr* and *sarA* leads to an almost avirulent behaviour and promotes a long term intracellular persistence [95]. However, usage of single mutants did not cause any differences in comparison to the other bacterial strains.

To exclude interfering effects of viral and bacterial infection, the experimental setting was simplified. Instead of the viral infection, stimulation with human IFNβ was likewise tested, since type I IFN leads to the induction of JAK-STAT signalling. For this latter setup, A549 cells were mock-treated or infected with *S. aureus* LS1 and SH1000 wt and mutant strains (ΔsigB, Δagr, ΔsarA, Δagr+ΔsarA) (MOI = 50) for 7.5h. Afterwards, the stimulation with IFNβ for 0.5h was performed and the phosphorylation patterns of STAT1 were monitored to possibly narrow down factors that could affect the signalling mechanisms on a molecular level.

The stimulation with IFNβ lead to a clear and strong pSTAT1 signal, while the co-stimulation with *S. aureus* SH1000 strain revealed a diminished expression, as expected (Fig. 6B). Nevertheless, infection with SH1000 double mutant strain (*agr* and *sarA*) didn't result in a stronger reduction of STAT1 phosphorylation as observed upon PR8M infection. Interestingly, usage of the *S. aureus* LS1 wt and mutant strains, resulted in a uniform and equal STAT1 phosphorylation on IFNβ-only and

IFNβ-*S. aureus* scenarios (Fig. 6C). These results indicate bacterial strain-dependent effects on the activated JAK-STAT pathway. Based on these findings, we were prompted to investigate if the *S. aureus* SH1000 strain is also able to impair the STAT1-STAT2 dimerization, that is essential for the expression of IFN-induced antiviral genes, as observed for *S. aureus* 6850.

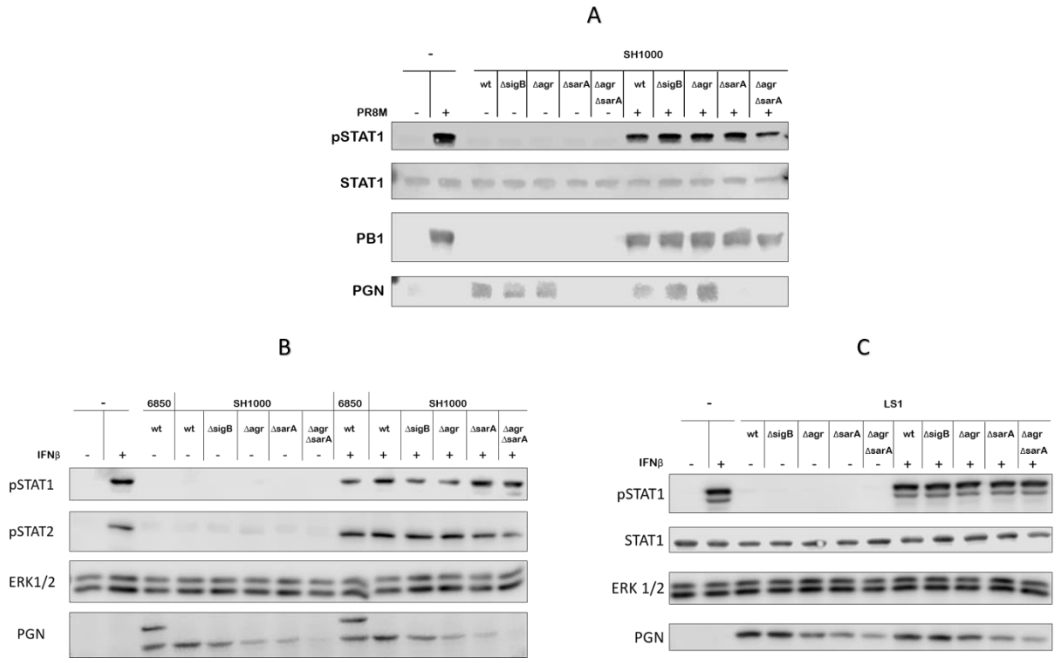

Fig. 6. The quality in reduction of influenza virus-induced STAT1 phosphorylation seems to be dependent on the bacterial strain. A549 cells were mock-treated or infected with PR8M (MOI = 5) for 8 h. Co-infection with *S. aureus* SH1000 wt and mutants (MOI = 50) was accomplished 30 min p.i. (A). A549 cells were mock-treated or infected with *S. aureus* SH1000 wt and mutants or LS1 wt and mutants (MOI = 50) for 7.5 h and subsequently stimulated with 500 U ml^{-1} human IFNβ for 30 min (B, C). Extracellular bacteria growth was stopped by a gentamicin treatment and a PBS wash step 3 h post bacterial infection. Whole cell lysates were subjected to WB analysis monitoring phosphorylated STAT1 (Y701), PB1 and PGN. STAT1 and ERK 1/2 were monitored as loading control. Data is representative of at least three independent experiments.

Using the protocol carried out successfully by Warnking and her colleagues [207], we advanced to the co-immunoprecipitation experiments with reduced scenarios due to the high costs of this method. We used the *S. aureus* SH1000 wt, *sigB* and *agr* mutant strains in detriment of *sarA* and the double mutant by relative importance in terms of impact on the bacterial virulence and mechanisms. Using *S. aureus* 6850 wt as positive control, it was possible to show that the *S. aureus* SH1000 wt and tested mutant strains (*sigB* and *agr*) reveal the same or even higher impact on STAT1-STAT2 dimerization as the *S. aureus* 6850 wt strain (Fig. 7A). In more detail, the measured relative intensity values of the bands reveal a significant decrease of STAT1 signal when the co-stimulation scenarios

are analysed (Fig. 7B). Interestingly, the *S. aureus* 6850 and SH1000 wt strains seem to possess similar abilities in down-regulation of IFN-induced signalling comparable to the mutant strains.

Another intriguing observation concerned the control of bacterial protein expression. Using an antibody which detects the peptidoglycan (PGN) polymer, an essential component of the bacterial cell envelope in both the gram-positive and gram-negative bacteria, a weaker signal for *agr* mutant strain is revealed (Fig. 7A). During experiments using the *S. aureus* 6850 strain, it was possible to capture the PGN signal (Fig. 5A). Similar was true for the *S. aureus* LS1 and SH1000 wt strains. However, detection of PGN upon infection with *S. aureus* mutant strains revealed less protein expression. Nevertheless, irrespective of the weaker signal for the *agr*, *sarA* and *agr+sarA* mutants, we were also able to reduce phosphorylation of STAT1 (Fig. 6B), as well as STAT1-STAT2 dimerization (Fig. 7).

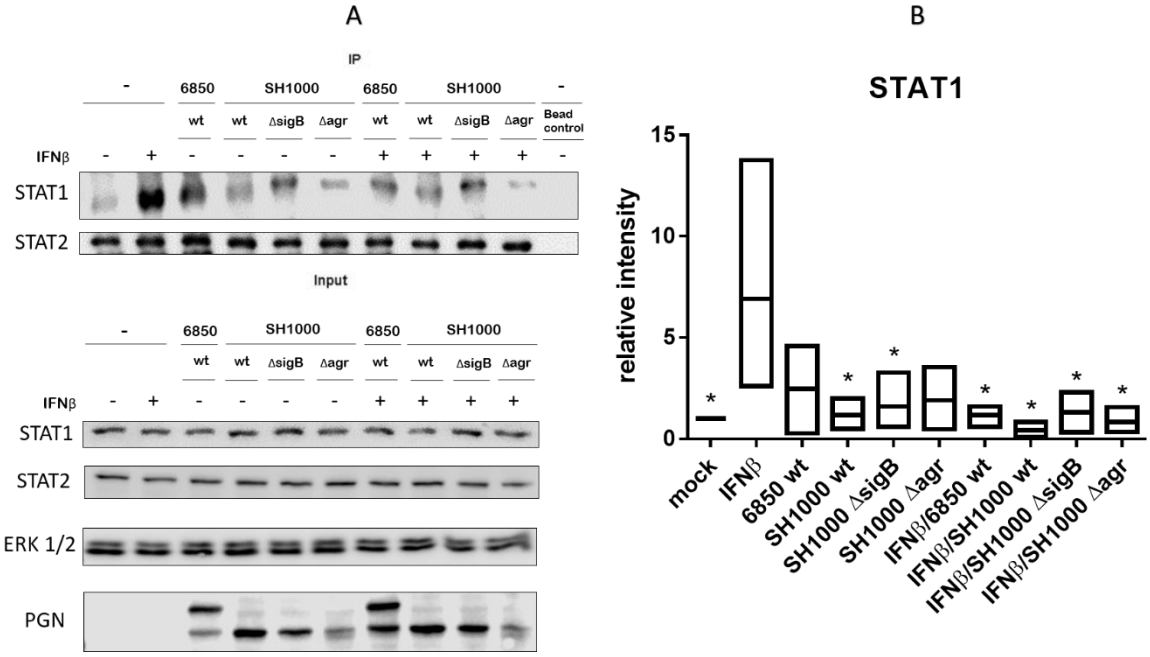

Fig. 7. IFNβ-induced signalling is inhibited in a co-stimulation scenario with *S. aureus* on the level of STAT1-STAT2 dimerization (A). A549 cells were mock-treated or infected with *S. aureus* 6850 wt or SH1000 wt and mutants (MOI = 50) for 2.5 h and subsequently stimulated with 100 U ml^{-1} human IFNβ for 30 min. Protein extracts were subjected to STAT2 immunoprecipitation (IP) followed by immunoblotting with STAT1. STAT2 expression was monitored as loading control. Relative levels of STAT1 were quantified by using Image Studio Lite Version 5.2 and normalized to STAT1 INPUT control (B). Data represent the means ± SD of at least three independent experiments. Statistical significance was evaluated by a one-way ANOVA followed by Dunnett's multiple comparison test (*P < 0.05) and differences are relative to IFNβ sample.

4.2 *S. aureus* SH1000 wild-type and mutant strains present different growth behaviour and contrasting capacity to infect

The observed decrease in the PGN signal for several of the mutants prompted us to investigate the influence of a hypothetical lower intracellular bacterial load upon infection with some of the *S. aureus* mutant strains. Firstly, we analysed the growth kinetics of each SH1000 strain, wt and mutants, for 12 h. The results indicate a standard growth behaviour for the *S. aureus* wt as well as the *S. aureus agr* and *agr+sarA* mutant strains (Fig. 8). However, the *S. aureus sigB* and *sarA* mutants show differences in growth. While *S. aureus sigB* mutant presents a very short exponential phase and an early stationary stage, the *S. aureus sarA* mutant displays a long log phase which is still going 12 h after inoculation (Fig. 8).

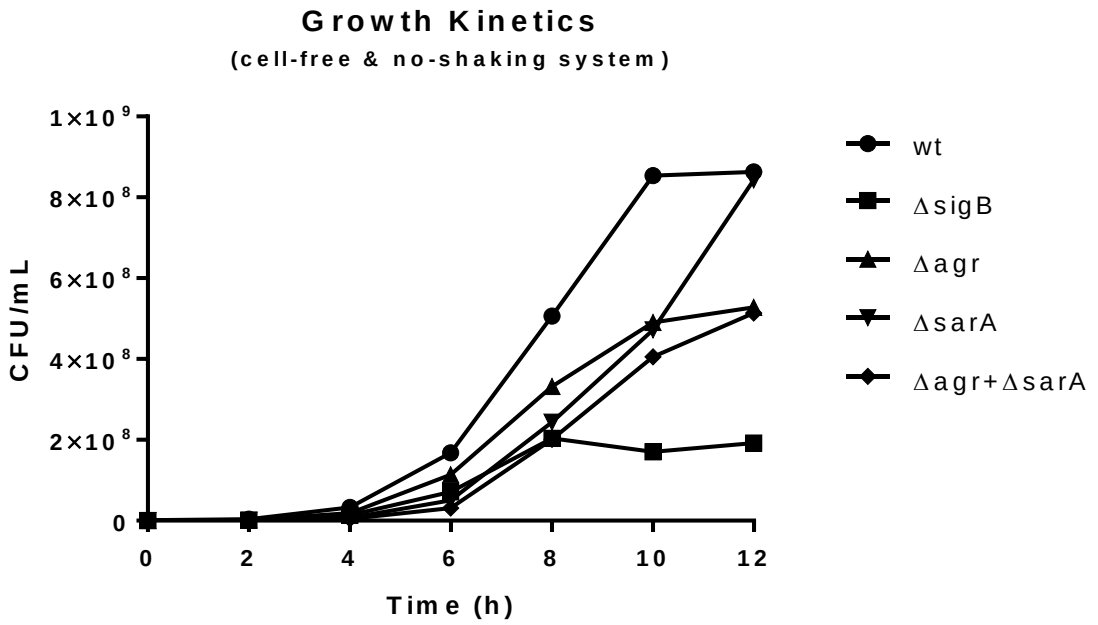

Fig. 8. The growth behaviour differs between the *S. aureus* SH1000 wt and mutant strains. 30 mL of Brain Heart Infusion (BHI) medium was inoculated with $1x10^6$ CFU ml^{-1} of each strain (SH1000 wt, ΔsigB, Δagr, ΔsarA, Δagr+ΔsarA) and incubated at 37°C for 12 h. A sample (1 mL) was collected for plating (40 µL) at 0, 2, 4, 6, 8, 10 and 12 h post inoculation. The OD_{600} was also measured at each hour post inoculation. Counting of colonies was performed the day after. Data represent the means of four independent experiments.

Further, it was important to dissect the amount of living bacteria that were, initially used for infection of cells. For this reason, a determination of the bacterial titres was performed by taking a sample of the overnight culture. Bacterial suspension was adjusted by a standard OD_{600} measurement (OD_{600} equal to 1 should mean $5x10^8$ CFU/mL) and subsequently plated. In

suspensions containing bacterial mutant strains, lower concentrations were measured in comparison to suspensions containing a bacterial wt strain. Furthermore, the expected growth value of $5x10^8$ living bacteria/mL was not achieved in presence of the bacterial mutants (Fig. 9). Based on these results, the infection doses were calculated exactly for each bacterial strain. To investigate the question if bacterial uptake and internalisation into cells was similar for the different *S. aureus* strains, intracellular bacterial titres were determined. In addition, the IAV and *S. aureus* co-infection was performed, as described above. While bacterial titres of single infection and co-infection with IAV did not differ significantly (Fig. 10), the SH1000 wt strain revealed a better capacity to infect lung cells than the bacterial mutant strains by one log (Fig. 10).

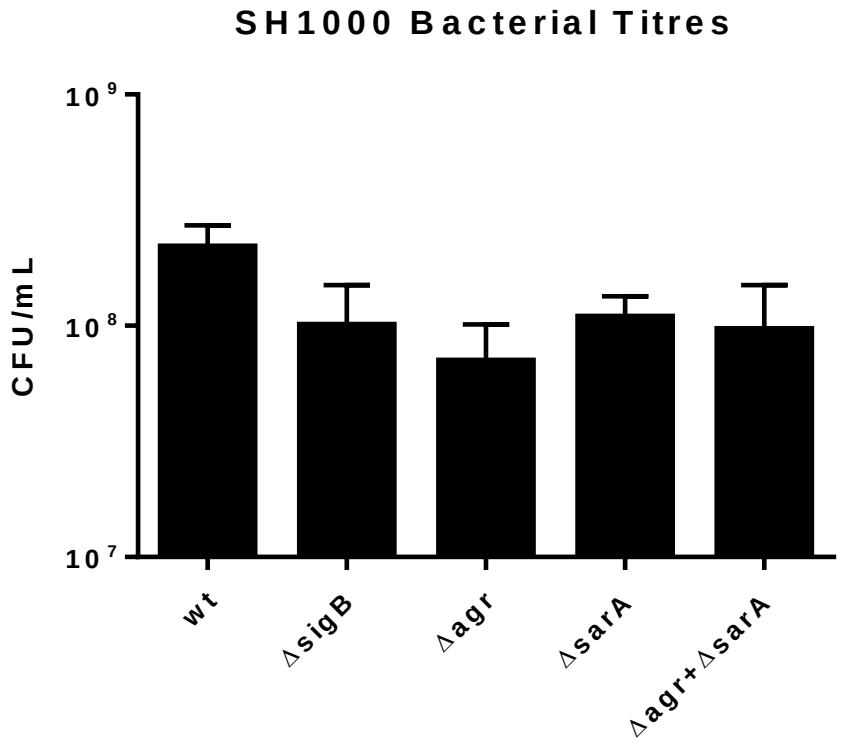

Fig. 9. The growth of SH1000 wt strain and the mutant strains still reveal slight differences when adjusted to OD_{600} = 1. Overnight cultures of the indicated bacteria (SH1000 wt, ΔsigB, Δagr, ΔsarA, Δagr+ΔsarA) were diluted with PBS to reach a standard value between 0.9 and 1.1, which should point to $5x10^8$ CFU mL^{-1}. From those adjusted cultures, subsequent dilutions and plating were performed. Counting of colonies was achieved the day after. Data represent the means of four independent experiments. Statistical significance was evaluated by a one-way ANOVA followed by Dunnett's multiple comparison test (*P < 0.05).

In summary, it became obvious that the *S. aureus* SH1000 wt strain presents a better fitness in terms of growth and capacity to infect cells in comparison to the mutant strains. Nevertheless, the

better growth capacity of the *S. aureus* SH1000 wt strain doesn't entirely explain the failure of PGN detection upon infection with some of the mutants, since each one of the *S. aureus* SH1000 strains was internalised and apparently capable of replicate with success.

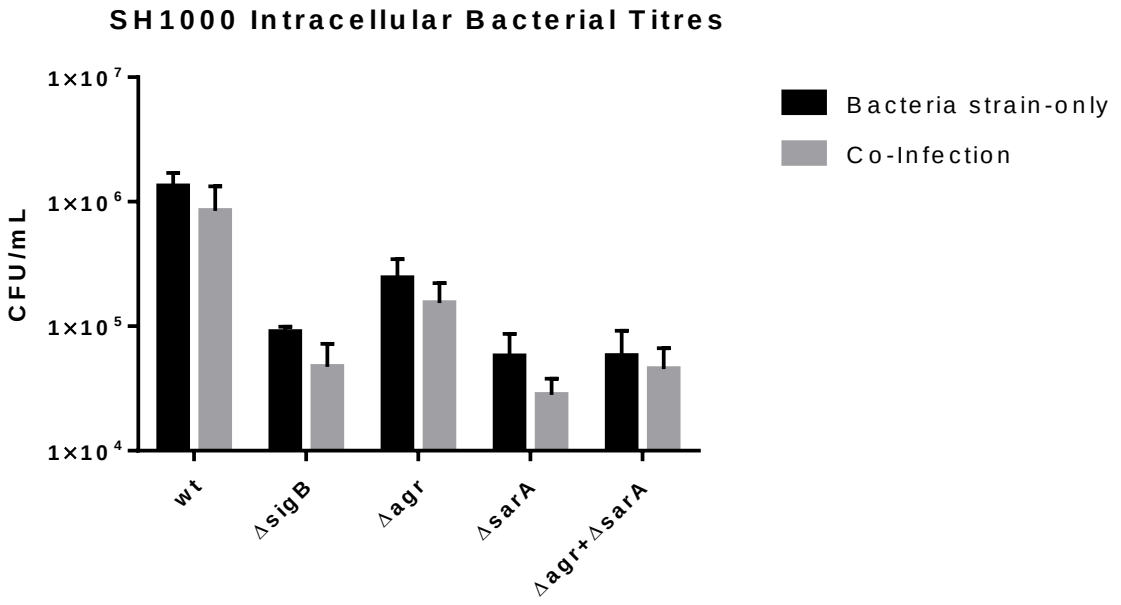

Fig. 10. SH1000 wt strain demonstrates a better capacity to infect human lung epithelial cells in relation to the mutant strains. A549 cells were mock-treated or infected with PR8M (MOI = 5) for 8 h (A). Co-infection with *S. aureus* SH1000 wt and mutants (SH1000 wt, ΔsigB, Δagr, ΔsarA, Δagr+ΔsarA) (MOI = 50) was accomplished 30 min p.i. Extracellular bacteria growth was stopped by a gentamicin treatment and a PBS wash step 3 h post bacterial infection. After 8 h, cells were lysed by osmotic shock, dilutions were performed, and bacteria were plated. Counting of bacteria was achieved the day after. Data represent the means of four independent experiments. Statistical significance was evaluated by a one-way ANOVA followed by Dunnett's multiple comparison test (*P < 0.05).

4.3 STAT1 phosphorylation is still inhibited upon adjustment of infection doses of bacterial mutants in co-infection scenario

To investigate how the growth differences between different bacterial strains affect type I IFN-induced signalling in presence of PR8M and different *S. aureus* SH1000 strains, pSTAT1 protein expression was examined upon co-infection. For this reason, the growth ability of different bacterial overnight culture was checked by determination of specific titres of each strain (Fig. 6). Instead of using $5x10^8$ CFU/mL for each strain the adapted concentrations were employed.

Co-infection with *S. aureus* resulted in a reduced pSTAT1 signal intensity with every SH1000 strain as well as an increase in the virus control protein (PB1) (Fig. 11). As before, it wasn't possible to

perceive *sarA* and *agr+sarA* PGN band. In summary, we could show that IAV-induced STAT1 phosphorylation is inhibited in presence of *S. aureus* but seems not to be dependent on specific mutations (Fig. 6A | Fig. 11).

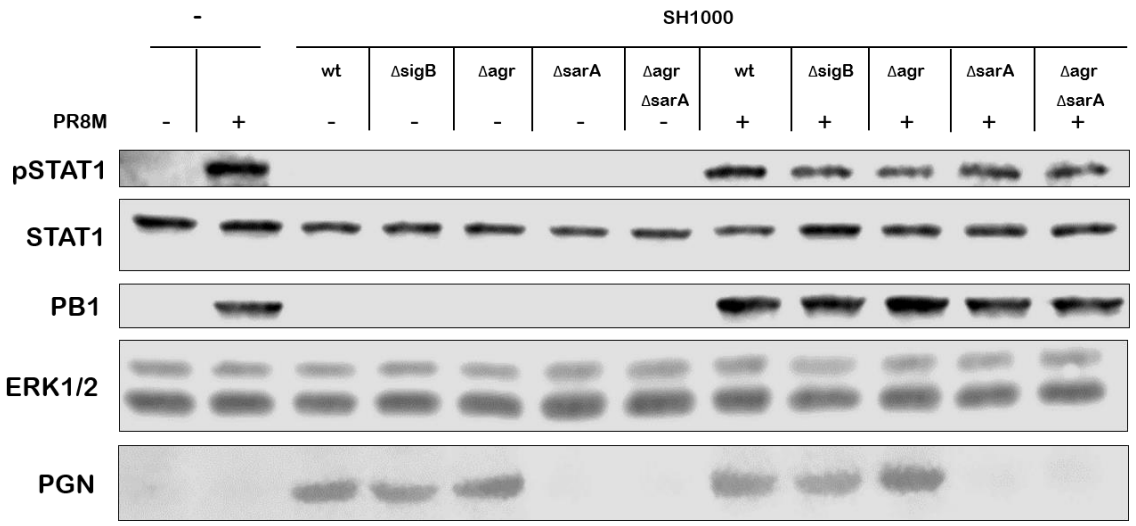

Fig. 11. Inhibition of influenza virus-induced STAT1 phosphorylation does not differ between the mutant strains upon bacterial adjustment. A549 cells were mock-treated or infected with PR8M (MOI = 5) for 8 h. Co-infection with *S. aureus* SH1000 wt and mutants (SH1000 wt, ΔsigB, Δagr, ΔsarA, Δagr+ΔsarA) (MOI=50) was accomplished 30 min p.i. Extracellular bacteria growth was stopped by a gentamicin treatment and a PBS wash step at 3 h post bacterial infection. Whole cell lysates were subjected to WB analysis monitoring phosphorylated STAT1 (Y701), PB1 and PGN. STAT1 and ERK 1/2 were monitored as loading control. Data are representative of at least three independent experiments.

4.4 IAV replication is increased in the presence of *S. aureus* SH1000

Increased pathogen load is one of the major causes of complications in co-infection scenarios and is responsible for the high morbidity and mortality rates [112].

To unravel the impact of various bacterial factors on viral replication, different *S. aureus* SH1000 mutant strains were used during IAV co-infection in comparison to the *S. aureus* SH1000 wt strain. After the first viral replication cycle, at 8 h upon IAV infection, progeny virus titres were analysed (Fig. 12). Not only in the presence of the *S. aureus* SH1000 wt strain but also in presence of the different *S. aureus* SH1000 mutant strains, even though to a lower extent, viral replication was increased. In presence of *S. aureus* wt, viral replication is 2.5-fold higher than in single IAV infection and still 1.6 – 2.1-fold higher in presence of the *S. aureus* mutant strains.

In summary, PR8M replication is enhanced in presence of *S. aureus* SH1000 wt and mutant strains. These results correlate to a former study by Warnking and colleagues [207], where the *S. aureus* 6850 wt strain was tested, resulting in an even higher effect on IAV replication.

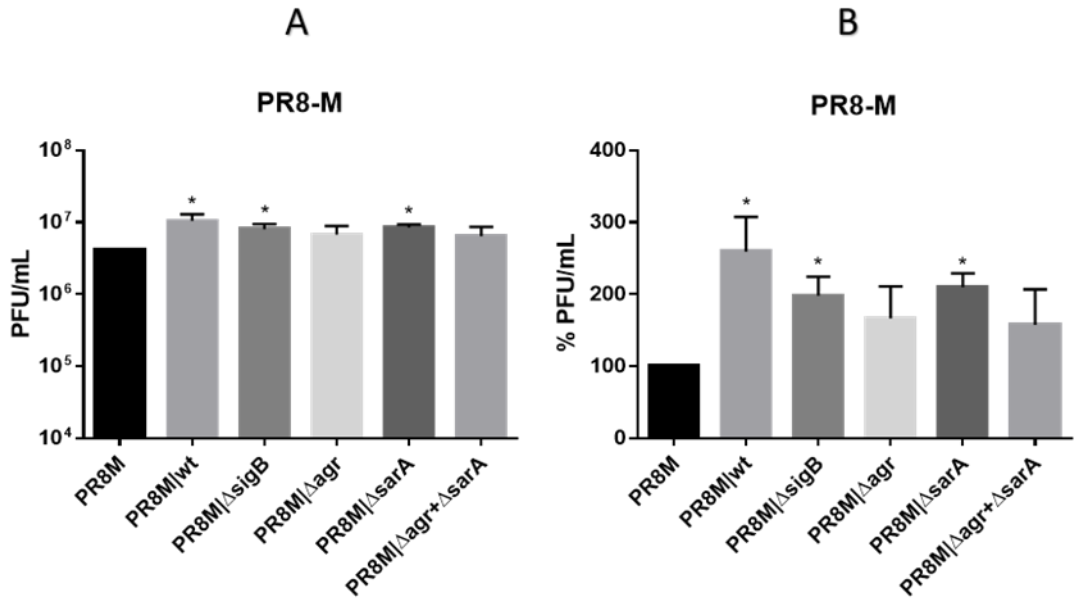

Fig. 12. Virus replication is increased in a co-infection scenario with the *S. aureus* SH1000 strain. A549 cells were mock-treated or infected with PR8M (MOI = 5) for 8 h. Co-infection with *S. aureus* SH1000 wt and mutants (SH1000 wt, ΔsigB, Δagr, ΔsarA, Δagr+ΔsarA) (MOI = 50) was accomplished 30 min p.i. Extracellular bacteria growth was stopped by a gentamicin treatment and a PBS wash step at 3 h post bacterial infection. The progeny virus titres were determined 8h p.i. by standard plaque assay. Results are depicted as PFU ml^{-1} (A) and n-fold of PR8M-only infected control (B). Data represent the means ± SD of at least three independent experiments. Statistical significance was evaluated by a one-way ANOVA followed by Dunnett's multiple comparison test (*P < 0.05).

4.5 Type I IFN-mediated ISG mRNA expression is reduced upon *S. aureus* co-infection

To get deeper insights in the mechanisms of *S. aureus*-mediated inhibition of IAV-induced type I IFN signalling, the induction of IFN stimulated genes (ISG) expression was measured on mRNA levels in presence and absence of SH1000 wt and mutant strains. Here, the *S. aureus* Δ*sarA* and Δ*agr*+Δ*sarA* mutants were again excluded due to difficulties in handling of the high number of biological and technical replicas and the the cost intensive experimental method. The investigation of SigB and Agr was included because *sigB* is most relevant for stress responses and *agr* for toxine production. As we are looking for a bacterial reaction upon challenge with an initial IAV infection, these two virulence regulators are the most appropriated and essential for this analysis.

While the virus control (M1 mRNA synthesis) revealed similar values for single and co-infection, the bacteria control (*aroE*) showed a slight increase in co-infection scenarios, as expected (Fig. 13). Moreover, co-infection with IAV and *S. aureus* strains resulted in a similar or slightly increased *IFNβ* mRNA expression, whereas *MxA* and *TRAIL* mRNA levels were reduced (Fig. 13).

Interestingly, upon infection with the *S. aureus* Δ*agr* mutant, the most significant decrease of *MxA* and *TRAIL* mRNA synthesis was observed, indicating an even more effective *S. aureus*-mediated inhibition of the innate gene expression when this gene is silenced.

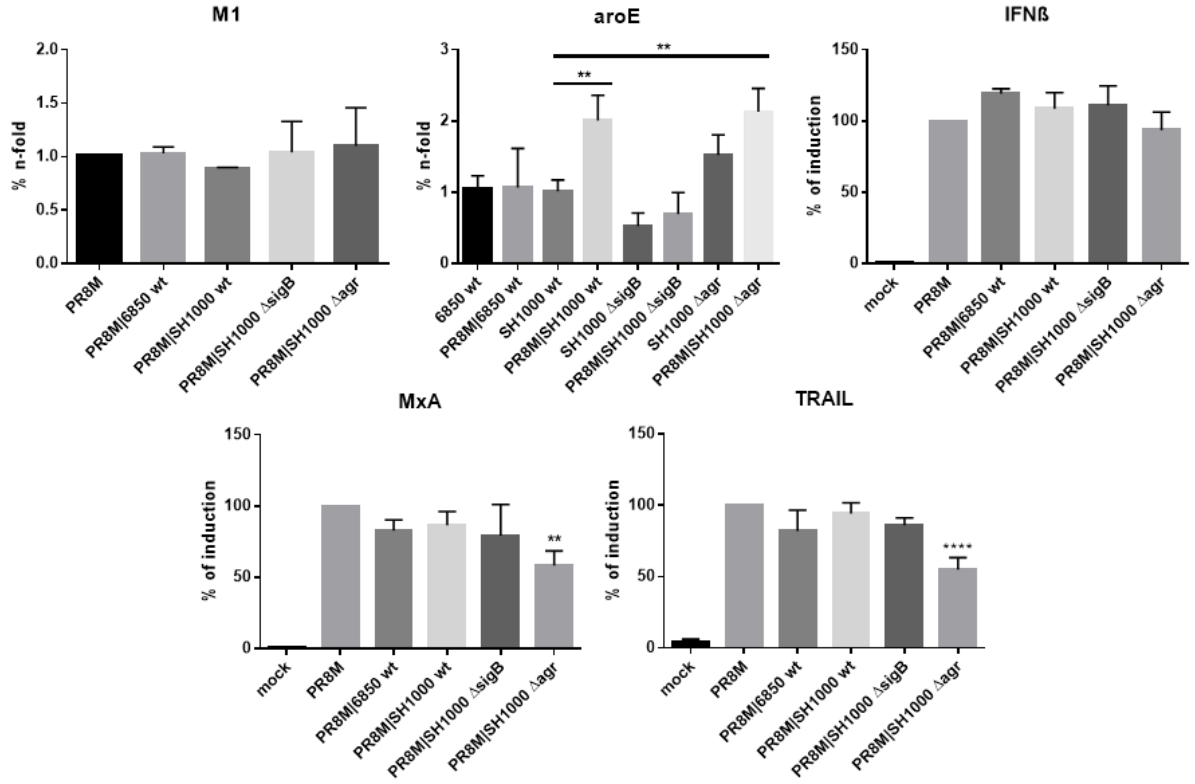

Fig. 13. Combined infection with influenza virus and *S. aureus* results in enhanced or equal *IFNβ* mRNA synthesis, but reduction of IFN-stimulated gene expression. A549 cells were infected with PR8M (MOI = 5) or were mock-treated. Co-infection with *S. aureus* 6850, SH1000 or mutants (Δ*sigB*, Δ*agr*) (MOI = 50) was accomplished 30 min p.i.. The growth of extracellular bacteria was stopped by gentamicin treatment 3 h post bacterial infection. After an additional PBS wash, cells were supplemented with fresh medium. Levels of *M1*, *aroE*, *IFNβ*, *MxA* and *TRAIL* mRNA were measured in duplicate by qRT-PCR at 8 h p.i. The PR8M-only infected samples were arbitrarily set as 100%. Data represent the means ± SD of at least three independent experiments. Statistical significance was evaluated by a one-way ANOVA followed by Dunnett's multiple comparison test (*P < 0.05; **P < 0.01; ***P < 0.001; ****P< 0.0001).

In summary, based on the results of IAV-*S. aureus* co-infection and IFNβ-*S. aureus* co-stimulation experiments we suppose a similar potency of *S. aureus* 6850 and SH1000 strains in contrast to the

LS1 strain regarding interference with type I IFN-mediated signalling. Nonetheless, the lack of *agr* expression, resulting in less ISG mRNA synthesis but higher bacterial load, indicated by higher *aroE* mRNA levels, the comparable effects on viral STAT1 phosphorylation as well as on viral replication might be a hint that a bacterial surface protein or another structural protein instead of a toxin is responsible for inhibition of type I IFN-mediated signalling.

5. Discussion

As stated in the project goals, the major aim of this study was to uncover a factor of S*. aureus* responsible for interference with type I IFN-mediated signalling inhibition. By using various *S. aureus* strains, including specific mutants, the focus was given on a particular step of the JAK-STAT pathway inhibition. The *S. aureus*-mediated inhibition of STAT1 and STAT2 dimerization was already shown to be a critical point for the unleashed immunopathology after a co-infection by Warnking and her colleagues [207]. They have shown an increased virus replication as well as a diminished ISG expression after challenging epithelial cells with both pathogens. Previous studies also demonstrate the necessity of a stable STAT1-STAT2 heterodimer for the nuclear translocation and efficient activation of gene expression [216,217].

5.1 *S. aureus*-mediated inhibition of type I IFN signalling seems to be strain-dependent

By use of an *in vitro* co-infection protocol [207], we verified that IAV-*S. aureus* co-infection as well as IFNβ-*S. aureus* co-stimulation lead to an dysregulation of immune response [143,207,218]. However, changes in cellular defence mechanisms seem to be dependent on the *S. aureus* strain used for infection (Fig.6). While similar features appear to be shared by *S. aureus* 6850 and SH1000 strains, the same can't be claimed for the *S. aureus* LS1 strain. Yet, a recent study analysed the host cell invasion of different strains on different cell types, which both included these three strains and the used cell line in this project [219]. Interestingly, only the *S. aureus* strain SH1000 reveals a reduced invasion capacity even though each bacterial strain tested induces inflammatory reaction, quickly after infection [219]. In addition, it is known that IAV infection results in disruption of epithelial cells barriers and tight junctions [220], which might support efficient bacterial internalization. Consequently, it is unlikely that the differences we observed on the ability to impair the type I IFN-mediated signalling is based on the invasion processes of the different strains.

Thus, specific characteristics of the different bacterial strains have to be considered. The *S. aureus* LS1 strain is known as an isolate from a swollen joint of a spontaneously arthritic mouse [221], encapsulated by capsular polysaccharide type 5 and expressing large amounts of toxic shock syndrome toxin 1 (TSST-1) [222]. In comparison to the laboratory strain *S. aureus* SH1000, the *S. aureus* LS1 isolate and *S. aureus* 6850 are more aggressive. Besides that, proteomic data unravelled strong cytotoxic factors of the *S. aureus* 6850 and LS1 strains, which are regulated by the *agr*-system [219,223]. A system that is less expressed in the *S. aureus* SH1000 strain [211]. Additionally, more resemblances

were noticed between *S. aureus* 6850 and LS1 strains, in contrast to *S. aureus* SH1000, when we investigated their virulence behaviour. However, neither *S. aureus* LS1 wt nor mutants (Δ*sigB*, Δ*agr*, Δ*sarA*, Δ*agr* + Δ*sarA*) were able to block the type I IFN-mediated signalling (Fig. 6C) as observed upon infection with *S. aureus* 6850 wt. Thus, none of the bacterial factors or the combination of factors of this strain, which were tested by use of mutants seems to alter type I IFN-mediated signalling, indicating to an independent process or factor. Another explanation might be a mechanism impairing the immune response autonomous of these tested factors.

In quite contrast, the use of *S. aureus* SH1000 indicated similar inhibitory effects by *S. aureus* wt and mutants during IAV co-infection or IFNβ co-stimulation. Even though it's possible to acknowledge more dissimilarities between the co-infection or co-stimulation scenarios, inhibition of the STAT1 phosphorylation was as effective in presence of bacterial mutant as in presence of wt strains (Figs. 6A, 6B | 7 | 11). Yet, a potential bacterial factor with impact on the immune response impairing would suggest a phosphorylation state similar to the IAV-only infection. In summary, the observed protein expression indicates a strain-specific aptitude that was not present or activated in presence of *S. aureus* LS1 due to differences upon mouse adaptation. Moreover, it is known that pathogenesis is critically determined by mutations in response to primal stimulus and a novel environment [224].

These findings are in line with the genetic reports stating a large host-specific relevance between *S. aureus* populations [225–227]. However, these host specific characteristics of *S. aureus* and its molecular basis are barely known, indicating the requirement of further knowledge of crucial genetic features that drive changes of the infection traits [228].

In summary, our data demonstrate an equal effectiveness of *S. aureus* 6850 and SH1000 strains on inhibition of type I IFN-mediated signalling, while *S. aureus* LS1 strains lacks this capability. Consequently, we propose a *S. aureus* strain specific-mediated impairment mechanism on the JAK-STAT pathway.

5.2 *Agr* silence results in a reduction of IAV-induced immune response

The *agr* regulon has been studied for over two decades because of its critical importance in *S. aureus* virulence. It is a well-known chromosomal locus responsible for the quorum sensing (QS), which induces the production and sensing of a diffusive molecule called autoinducing peptide (AIP). By AIP detection, bacteria knowledge about surrounding cell density is then acquired by this way of intercellular communication [229]. In like manner, virulence regulation operates based on this QS

circuit but regardless its value for virulence, it's not mandatory for the bacteria survival [95,230]. High genetic variability of *agr* [231], differences between clonal types due to mutations [232] and mutations emerging during the course of infection [233] were already reported. As a matter of fact, mutants are frequently detected in both asymptomatic carriers and severe infection patients, exposing an unclear vision of their role [234,235]. In general, a reduced cytotoxicity, but a better capacity to persist is stated to be the main advantage from this compromise [235,236].

Interestingly, in case of IAV and *S. aureus* co-infection, *S. aureus* SH1000 Δ*agr* mutant was able to downregulate IAV-induced ISGs mRNA levels (50%) in comparison to the single viral infection or co-infection with IAV and the bacterial wt strain (20%-30%) (Fig. 13). In addition, co-immunoprecipitation experiments show an almost complete block of the IAV-induced STAT1-STAT2 dimerization in presence of the *S. aureus* SH1000 Δ*agr* mutants (Fig. 7a). Furthermore, our data indicate the most similar growth kinetics as well as higher bacterial load in comparison to the *S. aureus* SH1000 wt strain (Fig. 8 and 13, respectively). To summarize, we were able to identify a bacterial strain that is more effective in the inhibition of the IAV-induced type I IFN signalling than the corresponding *S. aureus* wt strain.

Several studies introduced the *agr* dysfunction as the endpoint of a microevolution process within the host [236–238] and an enhanced ability to evade the host's immune system during infection [239,240], that might explain the strong inhibitory effects on anti-pathogen cellular functions.

5.3 Bacterial load doesn't correlate to the block of immune responses

One of the observations made during our experiments concerned the reduced PGN expression upon infection of A549 cells with different *S. aureus* mutants (*agr*, *sarA*, *agr+sarA*), indicating a lower bacterial load.

As expected, use of the *S. aureus* SH1000 mutant strains resulted in about one log reduction of intracellular bacterial titers compared to infection with the *S. aureus* SH1000 wt strain (Fig. 10). Upon adjustment of bacterial load, the *agr*-regulated changes in immune responses were comprised (Fig. 11 | 13). Another reason for the weakened PGN signal might be the overexpression of extracellular proteases and nucleases by the *sarA* mutant strains [241] that can interfere with the antibody recognition, leading to the outcome observed.

Additionally, post-invasion events can be considered as reason for *S. aureus*-mediated interference with immune signalling. Since around two decades ago, various reports document *S. aureus* survival

within several cell types [219,242–244] and its impact on the infection development [245]. Furthermore, the tested mutations are correlated to invasion processes [243,246]. Consequently, the results display that these virulence factors are supporting but are not essential to penetrate non-professional phagocytes, as epithelial cells.

Likewise, higher intracellular *S. aureus* numbers and higher epithelial cell death were already demonstrated [219]. Thus, the correlation of bacterial load and impairment of the IAV-induced type I IFN signalling. Highly hostile strains, with active cytotoxic action like *S. aureus* 6850 and LS1, were already shown to invade cells more efficiently than *S. aureus* SH1000 strain [219]. With this in mind, our data support that the impairment of inflammatory reaction is not based on differences in bacterial titres since *S. aureus* LS1 is not able trigger the JAK-STAT block at all (Fig. 6C) and infection with *S. aureus* 6850 results in similar effects as infection with *S. aureus* SH1000 (Fig. 7). Although *S. aureus* LS1 was not able to inhibit IAV-induced type I IFN response in the present infection scenario, we were able to verify the *S. aureus*-mediated block by use of the *S. aureus* 6850 strain (Fig. 7) as demonstrated by Warnking and her colleagues [207].

In contrast to the inexistent relevance of the bacterial load on the immune response, a correlation between bacterial and viral load can be presumed. In presence of the *S. aureus* SH1000 wt strain, viral titres are more enhanced in comparison to the presence of the mutant strains (Fig. 12), correlating to the bacterial load. Nevertheless, a translational study published that even without much variation in active viral replication, co-infection scenarios reveal a well-adjusted control of chemokines by targeting proteins responsible for the regulation of the JAK-STAT pathway [247]. The *S. aureus*-mediated interference with JAK-STAT signalling [207,247] as well as the great benefit for viral replication [207] are in line with the presented data of this study. Based on the higher invasive capacity of *S. aureus* 6850 in comparison to SH1000, it can be suggested that higher bacterial load also supports a more efficient viral replication. These data show that *S. aureus* SH1000 didn't possess the same capacity or, perhaps, sufficient intracellular load to improve IV replication in the same way. For example, in an Australian study on young children infected with respiratory syncytial virus (RSV) and *Streptococcus pneumoniae*, both pathogens seemed to better thrive when one was accompanied by the other but, commonly and most significantly, when bacteria levels were high [248]. Besides that, it is well known how bacteria benefit from viral primary infection (Fig. 13) [249] and, more recently, findings have shown that virus replication can as well profit of bacterial presence [207]. However, few take into account the differences in bacterial and viral load [250,251] and its impact

on the host cell response. Therefore, it would be important to address this variables that can alter the disease outcome in a near future.

5.4 Perspectives on the elucidation of *S. aureus*-mediated interference with STAT1-STAT2 dimerization

While considering several hypotheses that were discussed in previous pages regarding both pathogens and their mechanisms on a co-infection scenario, another important aim of this study was to identify a *S. aureus* factor or *S. aureus*-controlled mechanism responsible for the regulation of the blockade of JAK-STAT signalling. Although a specific bacterial factor or mechanism was not identified so far, numerous steps towards that goal were achieved. Among these, various *S. aureus* strains and mutants, which are frequently used in laboratorial environments to study *S. aureus* pathogenesis, were employed in *in vitro* co-infection scenarios, for the first time. Consequently, studying the relevance of these bacterial mutants on the STAT1-STAT2 impairment was in the focus of interest. Especially the use of *S. aureus* SH1000 mutant strains lacking three important virulence regulators was most promising since Warnking and her colleagues already excluded the possibility of "inactivated bacteria and stimulation with different cell wall components, toxins or bacterial supernatant" to cause this inhibition of this primary innate antiviral system [207].

Nonetheless, it was possible to comprehend that none of the factors tested by use of the *S. aureus* SH1000 mutants seems to be responsible for the control of the STAT1-STAT2 dimerization. We could attain other conclusions discussed previously, but we showed clearly and with several methods that other mechanisms must be taken into account regarding this problem. STAT1 and STAT2 dimerization is impaired in presence of *S. aureus* infection and its molecular system capacity to manage that link is, undoubtedly, mastered as it keeps its effectivity with the knockout of crucial virulence factors. At the present time, as technology evolves, investigations beyond protein-protein interaction have to be performed with focus on host cell factors responsible for regulation of STAT1-STAT2 dimerization.

Equally important will be the deeper look onto other *S. aureus* factors that might be responsible for inhibition of type I IFN-mediated signalling. Provided that, a bacterial surface protein or another structural protein might be the relevant factor and not a toxin as initially expected. Accordingly, other organisms might be used for infection to further investigate pathogen-mediated interference with JAK-STAT signalling. Within a recent report of Sendai virus infections, the virus mediated inhibition of STAT1 and STAT2 phosphorylation was demonstrated [252]. Here, one single molecule of

Y3 (C-terminal half of a C viral protein – proteins responsible for anti-IFN function of the genera *Respirovirus* and *Morbillivirus*) was identified for the association with the heterodimer and posterior dephosphorylation. Additionally, it is curious to notice the high basicity of C viral proteins, a characteristic shared by the non-structural protein NS1, a basic IAV protein that also fulfils anti-IFN functions [253]. Based on these similarities, it would be interesting to investigate if NS1 is able to inhibit STAT1-STAT2 dimerization.

Another key point that is important to mention addresses longer timepoints (several days) in co-infection scenarios *i*n vivo, which reveal contrasting behaviours of STAT1 signalling during single influenza infections and co-infections. Numerous reports demonstrate that type I IFN-induced STAT1 activation impairs development of T-helper 17 (Th17) cells and plays a detrimental role in case of bacterial challenge [254–257]. Since Th17 cells are important mediators of neutrophilic responses in the lung, its suppression, due to primary viral infection, may culminate in a secondary bacterial pneumonia [258]. In detail, primary viral infection primes the immune system to upregulate antiviral genes, but results in downregulation of antiviral defence mechanisms responsible for clearing the virus particles from the host. During this process, Th17 immune activation is impaired by STAT1. With this in mind, the question arises why *S. aureus* promotes the host to deal effectively with the secondary bacterial infection? The most important function of activated STAT1 is to trigger antiviral defence against IAV infection, which is amplified by ISG induction. Anyway, IAVs are able to impede ISG transcription, replicate more efficiently and, apparently, turn the attention of the host immune system to the bacteria clearance. Thus, the responses to different pathogens are diverse and the creation of a balanced immune response on the course of varied infections is difficult. Reasonable answers to the question why *S. aureus* inhibits antiviral defence but promotes cellular mechanisms responsible for bacterial clearance might be due to times and complexity of *in vivo* infection, which further can alter drastically the inflammatory scenario [258]. Furthermore, the Th17 cell-mediated autoimmune inflammation can lead to serious lung injuries and syndromes [259,260]. During co-infection, Th17 responses are exacerbated in comparison to a control situation due to STAT1 dephosphorylation. Under those circumstances, it could lead to a reduced LD_{50} (median lethal dose) to influenza, increased morbidity and marked granulocytic pulmonary infiltration [261]. Throughout an ongoing infection, defence mechanisms are dynamic and progressively dealing with different challenges.

After IAV infection, type I IFN-mediated signalling is well studied and documented. However, the examination of molecular processes in an IAV/*S. aureus* co-infection scenario is still an evolving

process. Within the present study, we analysed the period until the end of first IAV replication (8h p.i.) and focused on *S. aureus*-mediated support of IAV survival. We were able to verify the data by Warnking and colleagues [207] and showed that the potency to inhibit the IAV-induced type I IFN response differs among the *S. aureus* strains and depend on different *S. aureus* virulence regulators. Furthermore, our data point to the importance of bacterial structural factors unrelated to virulence regulators within these processes that have to be studied by more sensitive methods in future analysis. As proteomics-based signalling research develops and bioinformatics tools are integrated, great potential and utility is expected from future projects to unravel the molecular cascades and signalling pathways in complex infections. This would prompt an improved disease diagnosis and enhanced therapeutic development for future populations.

6. Bibliography

1. Bakaletz, L. O. Developing animal models for polymicrobial diseases. *Nat. Rev. Microbiol.* **2,** 552–568 (2004).

2. Morens, D. M., Taubenberger, J. K. & Fauci, A. S. Predominant Role of Bacterial Pneumonia as a Cause of Death in Pandemic Influenza: Implications for Pandemic Influenza Preparedness. *J. Infect. Dis.* **198,** 962–970 (2008).

3. Robertson, L., Caley, J. P. & Moore, J. Importance of *Staphylococcus aureus* in pneumonia in the 1957 epidemic of influenza A. *Lancet (London, England)* **2,** 233–6 (1958).

4. McCullers, J. A. Insights into the interaction between influenza virus and pneumococcus. *Clin. Microbiol. Rev.* **19,** 571–582 (2006).

5. Klugman, K. P. & Madhi, S. A. Pneumococcal Vaccines and Flu Preparedness. *Science (80-.).* **316,** 49c–50c (2007).

6. Holland, T. L., Arnold, C. & Fowler, V. G. Clinical Management of *Staphylococcus aureus* Bacteremia. *JAMA* **312,** 1330–41 (2014).

7. Kohanski, M. A., Dwyer, D. J. & Collins, J. J. How antibiotics kill bacteria: from targets to networks. *Nat. Rev. Microbiol.* **8,** 423–435 (2010).

8. Tong, S. Y. C. *et al. Staphylococcus aureus* infections: epidemiology, pathophysiology, clinical manifestations, and management. *Clin. Microbiol. Rev.* **28,** 603–61 (2015).

9. Hodille, E. *et al.* The Role of Antibiotics in Modulating Virulence in *Staphylococcus aureus*. *Clin. Microbiol. Rev.* **30,** 887–917 (2017).

10. Houser, K. & Subbarao, K. Influenza Vaccines: Challenges and Solutions. *Cell Host Microbe* **17,** 295–300 (2015).

11. Shaw, M. L. & Palese, P. *Orthomyxoviridae*: The viruses and their replication. *Fields Virology* 1647–1689 (2007). doi:10.1016/0038-092X(88)90131-4

12. Kapoor, S. & Dhama, K. Properties of Influenza Viruses. in *Insight into Influenza Viruses of Animals and Humans* 7–13 (Springer International Publishing, 2014). doi:10.1007/978-3-319-05512-1_2

13. Bouvier, N. M. & Palese, P. The biology of influenza viruses. *Vaccine* **26 Suppl 4,** D49-53 (2008).

14. Hause, B. M. *et al.* Characterization of a novel influenza virus in cattle and Swine: proposal for a new

genus in the *Orthomyxoviridae* family. *MBio* **5,** e00031-14 (2014).

15. Webster, R. G., Bean, W. J., Gorman, O. T., Chambers, T. M. & Kawaoka, Y. Evolution and ecology of influenza A viruses. *Microbiol. Rev.* **56,** 152–79 (1992).

16. Iuliano, A. D. *et al.* Estimates of global seasonal influenza-associated respiratory mortality: a modelling study. *Lancet* **391,** 1285–1300 (2018).

17. Greenbaum, B. D., Li, O. T. W., Poon, L. L. M., Levine, A. J. & Rabadan, R. Viral reassortment as an information exchange between viral segments. *Proc. Natl. Acad. Sci. U. S. A.* **109,** 3341–6 (2012).

18. Matsuoka, Y. *et al.* A comprehensive map of the influenza A virus replication cycle. *BMC Syst. Biol.* **7,** 1 (2013).

19. Noda, T. Native morphology of influenza virions. *Front. Microbiol.* **2,** 1–5 (2012).

20. Skehel, J. J. & Hay, A. J. Nucleotide sequences at the 5’ termini of influenza virus RNAs and their transcripts. *Nucleic Acids Res.* **5,** 1207–19 (1978).

21. Robertson, J. S. 5’ and 3’ terminal nucleotide sequences of the RNA genome segments of influenza virus. *Nucleic Acids Res.* **6,** 3745–57 (1979).

22. Compans, R. W., Content, J. & Duesberg, P. H. Structure of the ribonucleoprotein of influenza virus. *J. Virol.* **10,** 795–800 (1972).

23. Heggeness, M. H., Smith, P. R., Ulmanen, I., Krug, R. M. & Choppin, P. W. Studies on the helical nucleocapsid of influenza virus. *Virology* **118,** 466–70 (1982).

24. Ruigrok, R. W. H. & Baudin, F. Structure of influenza virus ribonucleoprotein particles. II. Purified RNA-free influenza virus ribonucleoprotein forms structures that are indistinguishable from the intact influenza virus ribonucleoprotein particles. *J. Gen. Virol.* **76,** 1009–1014 (1995).

25. Zheng, W. & Tao, Y. J. Structure and assembly of the influenza A virus ribonucleoprotein complex. *FEBS Lett.* **587,** 1206–1214 (2013).

26. Stevens, J. *et al.* Structure of the Uncleaved Human H1 Hemagglutinin from the Extinct 1918 Influenza Virus. *Science (80-.).* **303,** 1866–1870 (2004).

27. Varghese, J. N., Laver, W. G. & Colman, P. M. Structure of the influenza virus glycoprotein antigen neuraminidase at 2.9 Å resolution. *Nature* **303,** 35–40 (1983).

28. Schnell, J. R. & Chou, J. J. Structure and mechanism of the M2 proton channel of influenza A virus. *Nature* **451,** 591–595 (2008).

29. Calder, L. J., Wasilewski, S., Berriman, J. A. & Rosenthal, P. B. Structural organization of a filamentous influenza A virus. *Proc. Natl. Acad. Sci.* **107,** 10685–10690 (2010).

30. Fouchier, R. A. M. *et al.* Characterization of a Novel Influenza A Virus Hemagglutinin Subtype (H16) Obtained from Black-Headed Gulls. *J. Virol.* **79,** 2814–2822 (2005).

31. Wu, Y., Wu, Y., Tefsen, B., Shi, Y. & Gao, G. F. Bat-derived influenza-like viruses H17N10 and H18N11. *Trends Microbiol.* **22,** 183–191 (2014).

32. Bui, M., Wills, E. G., Helenius, A. & Whittaker, G. R. Role of the influenza virus M1 protein in nuclear export of viral ribonucleoproteins. *J. Virol.* **74,** 1781–6 (2000).

33. Noton, S. L. *et al.* Identification of the domains of the influenza A virus M1 matrix protein required for NP binding, oligomerization and incorporation into virions. *J. Gen. Virol.* **88,** 2280–2290 (2007).

34. Hutchinson, E. C. *et al.* Conserved and host-specific features of influenza virion architecture. *Nat. Commun.* **5,** 4816 (2014).

35. García-Sastre, A. Induction and evasion of type I interferon responses by influenza viruses. *Virus Res.* **162,** 12–18 (2011).

36. Ehrhardt, C. *et al.* Interplay between influenza A virus and the innate immune signaling. *Microbes Infect.* **12,** 81–87 (2010).

37. Richardson, J. C. & Akkina, R. K. NS2 protein of influenza virus is found in purified virus and phosphorylated in infected cells. *Arch. Virol.* **116,** 69–80 (1991).

38. Klemm, C., Boergeling, Y., Ludwig, S. & Ehrhardt, C. Immunomodulatory Nonstructural Proteins of Influenza A Viruses. *Trends Microbiol.* **26,** 624–636 (2018).

39. Connor, R. J., Kawaoka, Y., Webster, R. G. & Paulson, J. C. Receptor Specificity in Human, Avian, and Equine H2 and H3 Influenza Virus Isolates. *Virology* **205,** 17–23 (1994).

40. Helenius, A. Unpacking the incoming influenza virus. *Cell* **69,** 577–8 (1992).

41. Fodor, E. & Smith, M. The PA subunit is required for efficient nuclear accumulation of the PB1 subunit of the influenza A virus RNA polymerase complex. *J. Virol.* **78,** 9144–53 (2004).

42. Deng, T., Sharps, J., Fodor, E. & Brownlee, G. G. In Vitro Assembly of PB2 with a PB1-PA Dimer Supports a New Model of Assembly of Influenza A Virus Polymerase Subunits into a Functional Trimeric Complex. *J. Virol.* **79,** 8669–8674 (2005).

43. Resa-Infante, P. *et al.* The Host-Dependent Interaction of α-Importins with Influenza PB2

Polymerase Subunit Is Required for Virus RNA Replication. *PLoS One* **3,** e3904 (2008).

44. Neumann, G., Brownlee, G. G., Fodor, E. & Kawaoka, Y. Orthomyxovirus replication, transcription, and polyadenylation. *Curr. Top. Microbiol. Immunol.* **283,** 121–43 (2004).

45. Ulmanen, I., Broni, B. A. & Krug, R. M. Role of two of the influenza virus core P proteins in recognizing cap 1 structures (m7GpppNm) on RNAs and in initiating viral RNA transcription. *Proc. Natl. Acad. Sci. U. S. A.* **78,** 7355–9 (1981).

46. Blaas, D., Patzelt, E. & Kuechler, E. Identification of the cap binding protein of influenza virus. *Nucleic Acids Res.* **10,** 4803–12 (1982).

47. Blaas, D., Patzelt, E. & Kuechler, E. Cap-recognizing protein of influenza virus. *Virology* **116,** 339–48 (1982).

48. Braam, J., Ulmanen, I. & Krug, R. M. Molecular model of a eucaryotic transcription complex: Functions and movements of influenza P proteins during capped RNA-primed transcription. *Cell* **34,** 609–618 (1983).

49. Pflug, A., Lukarska, M., Resa-Infante, P., Reich, S. & Cusack, S. Structural insights into RNA synthesis by the influenza virus transcription-replication machine. *Virus Res.* **234,** 103–117 (2017).

50. Klenk, H.-D., Wagner, R., Heuer, D. & Wolff, T. Importance of hemagglutinin glycosylation for the biological functions of influenza virus. *Virus Res.* **82,** 73–5 (2002).

51. Wagner, R., Matrosovich, M. & Klenk, H.-D. Functional balance between haemagglutinin and neuraminidase in influenza virus infections. *Rev. Med. Virol.* **12,** 159–166 (2002).

52. Wang, P., Palese, P. & O'Neill, R. E. The NPI-1/NPI-3 (karyopherin alpha) binding site on the influenza a virus nucleoprotein NP is a nonconventional nuclear localization signal. *J. Virol.* **71,** 1850–6 (1997).

53. Nieto, A., de la Luna, S., Barcena, J., Portela, A. & Ortin, J. Complex structure of the nuclear translocation signal of influenza virus polymerase PA subunit. *J. Gen. Virol.* **75,** 29–36 (1994).

54. Hutchinson, E. C., Orr, O. E., Man Liu, S., Engelhardt, O. G. & Fodor, E. Characterization of the interaction between the influenza A virus polymerase subunit PB1 and the host nuclear import factor Ran-binding protein 5. *J. Gen. Virol.* **92,** 1859–1869 (2011).

55. Ye, Z., Robinson, D. & Wagner, R. R. Nucleus-targeting domain of the matrix protein (M1) of influenza virus. *J. Virol.* **69,** 1964–70 (1995).

56. Greenspan, D. *et al.* Expression of influenza virus NS2 nonstructural protein in bacteria and localization of NS2 in infected eucaryotic cells. *J. Virol.* **54,** 833–43 (1985).

57. Greenspan, D., Palese, P. & Krystal, M. Two nuclear location signals in the influenza virus NS1 nonstructural protein. *J. Virol.* **62,** 3020–6 (1988).

58. Schneider, J. & Wolff, T. Nuclear functions of the influenza A and B viruses NS1 proteins: do they play a role in viral mRNA export? *Vaccine* **27,** 6312–6 (2009).

59. Wu, C.-Y., Jeng, K.-S. & Lai, M. M.-C. The SUMOylation of Matrix Protein M1 Modulates the Assembly and Morphogenesis of Influenza A Virus. *J. Virol.* **85,** 6618–6628 (2011).

60. Pohl, M. O., Lanz, C. & Stertz, S. Late stages of the influenza A virus replication cycle—a tight interplay between virus and host. *J. Gen. Virol.* **97,** 2058–2072 (2016).

61. Gao, S. *et al.* Interaction of NS2 with AIMP2 facilitates the switch from ubiquitination to SUMOylation of M1 in influenza A virus-infected cells. *J. Virol.* **89,** 300–11 (2015).

62. Barman, S. *et al.* Role of transmembrane domain and cytoplasmic tail amino acid sequences of influenza a virus neuraminidase in raft association and virus budding. *J. Virol.* **78,** 5258–69 (2004).

63. Zhang, J. & Lamb, R. A. Characterization of the membrane association of the influenza virus matrix protein in living cells. *Virology* **225,** 255–66 (1996).

64. McCown, M. F. & Pekosz, A. The influenza A virus M2 cytoplasmic tail is required for infectious virus production and efficient genome packaging. *J. Virol.* **79,** 3595–605 (2005).

65. Rossman, J. S., Jing, X., Leser, G. P. & Lamb, R. A. Influenza Virus M2 Protein Mediates ESCRT-Independent Membrane Scission. *Cell* **142,** 902–913 (2010).

66. Palese, P., Tobita, K., Ueda, M. & Compans, R. W. Characterization of temperature sensitive influenza virus mutants defective in neuraminidase. *Virology* **61,** 397–410 (1974).

67. Bischoff, W. E., Reid, T., Russell, G. B. & Peters, T. R. Transocular Entry of Seasonal Influenza-Attenuated Virus Aerosols and the Efficacy of N95 Respirators, Surgical Masks, and Eye Protection in Humans. *J. Infect. Dis.* **204,** 193–199 (2011).

68. Institute of Medicine (US). *Preventing Transmission of Pandemic Influenza and Other Viral Respiratory Diseases*. *Preventing Transmission of Pandemic Influenza and Other Viral Respiratory Diseases: Personal Protective Equipment for Healthcare Personnel: Update 2010* (National Academies Press (US), 2011). doi:10.17226/13027

69. Paules, C. & Subbarao, K. Influenza. *Lancet* **390,** 697–708 (2017).

70. Lau, L. L. H. *et al.* Viral Shedding and Clinical Illness in Naturally Acquired Influenza Virus Infections. *J. Infect. Dis.* **201,** 1509–1516 (2010).

71. Ip, D. K. M. *et al.* The Dynamic Relationship Between Clinical Symptomatology and Viral Shedding in Naturally Acquired Seasonal and Pandemic Influenza Virus Infections. *Clin. Infect. Dis.* **62,** civ909 (2015).

72. Taubenberger, J. K. & Kash, J. C. Influenza Virus Evolution, Host Adaptation, and Pandemic Formation. *Cell Host Microbe* **7,** 440–451 (2010).

73. Maines, T. R. *et al.* Pathogenesis of emerging avian influenza viruses in mammals and the host innate immune response. *Immunol. Rev.* **225,** 68–84 (2008).

74. Cummins, C. S. & Harris, H. The Chemical Composition of the Cell Wall in some Gram-positive Bacteria and its Possible Value as a Taxonomic Character. *J. Gen. Microbiol.* **14,** 583–600 (1956).

75. Baird-Parker, A. C. A Classification of Micrococci and Staphylococci Based on Physiological and Biochemical Tests. *J. Gen. Microbiol.* **30,** 409–427 (1963).

76. Lory, S. The Family *Staphylococcaceae*. in *The Prokaryotes* 363–366 (Springer Berlin Heidelberg, 2014). doi:10.1007/978-3-642-30120-9_350

77. Finkelstein, R. A. & Sulkin, S. E. Characteristics of coagulase positive and coagulase negative staphylococci in serum-soft agar. *J. Bacteriol.* **75,** 339–44 (1958).

78. Sperber, W. H. & Tatini, S. R. Interpretation of the tube coagulase test for identification of *Staphylococcus aureus*. *Appl. Environ. Microbiol.* **29,** 502–5 (1975).

79. Yazdankhah, S. P. & Olsen, E. Simple and direct detection of *Staphylococcus aureus* in milk by a tube coagulase test. *Lett. Appl. Microbiol.* **27,** 111–5 (1998).

80. Archer, G. L. *Staphylococcus aureus*: a well-armed pathogen. *Clin. Infect. Dis.* **26,** 1179–81 (1998).

81. Lindsay, J. A. & Holden, M. T. G. *Staphylococcus aureus* : superbug, super genome? *Trends Microbiol.* **12,** 378–385 (2004).

82. Lynch, J. P. Hospital-acquired pneumonia: risk factors, microbiology, and treatment. *Chest* **119,** 373S–384S (2001).

83. Lowy, F. D. *Staphylococcus aureus* Infections. *N. Engl. J. Med.* **339,** 520–532 (1998).

84. Watts, A. *et al. Staphylococcus aureus* Strains That Express Serotype 5 or Serotype 8 Capsular Polysaccharides Differ in Virulence. *Infect. Immun.* **73,** 3502–3511 (2005).

85. Weidenmaier, C. & Peschel, A. Teichoic acids and related cell-wall glycopolymers in Gram-positive physiology and host interactions. *Nat. Rev. Microbiol.* **6,** 276–287 (2008).

86. Reichmann, N. T. & Gründling, A. Location, synthesis and function of glycolipids and polyglycerolphosphate lipoteichoic acid in Gram-positive bacteria of the phylum Firmicutes. *FEMS Microbiol. Lett.* **319,** 97–105 (2011).

87. Zapun, A., Contreras-Martel, C. & Vernet, T. Penicillin-binding proteins and β-lactam resistance. *FEMS Microbiol. Rev.* **32,** 361–385 (2008).

88. Patti, J. M., Allen, B. L., McGavin, M. J. & Hook, M. MSCRAMM-Mediated Adherence of Microorganisms to Host Tissues. *Annu. Rev. Microbiol.* **48,** 585–617 (1994).

89. Montoya, M. & Gouaux, E. Beta-barrel membrane protein folding and structure viewed through the lens of alpha-hemolysin. *Biochim. Biophys. Acta* **1609,** 19–27 (2003).

90. Niemann, S. *et al.* Combined Action of Influenza Virus and *Staphylococcus aureus* Panton–Valentine Leukocidin Provokes Severe Lung Epithelium Damage. *J. Infect. Dis.* **206,** 1138–1148 (2012).

91. Chesney, P. J., Bergdoll, M. S., Davis, J. P. & Vergeront, J. M. The Disease Spectrum, Epidemiology, and Etiology of Toxic-Shock Syndrome. *Annu. Rev. Microbiol.* **38,** 315–338 (1984).

92. Pinchuk, I. V., Beswick, E. J. & Reyes, V. E. Staphylococcal Enterotoxins. *Toxins (Basel).* **2,** 2177–2197 (2010).

93. Lowy, F. D. Is *Staphylococcus aureus* an intracellular pathogen? *Trends Microbiol.* **8,** 341–3 (2000).

94. Löffler, B., Tuchscherr, L., Niemann, S. & Peters, G. *Staphylococcus aureus* persistence in non-professional phagocytes. *Int. J. Med. Microbiol.* **304,** 170–176 (2014).

95. Tuchscherr, L. *et al.* Sigma Factor SigB Is Crucial to Mediate *Staphylococcus aureus* Adaptation during Chronic Infections. *PLoS Pathog.* **11,** (2015).

96. Mäder, U. *et al. Staphylococcus aureus* Transcriptome Architecture: From Laboratory to Infection-Mimicking Conditions. *PLOS Genet.* **12,** e1005962 (2016).

97. Pané-Farré, J., Jonas, B., Förstner, K., Engelmann, S. & Hecker, M. The σB regulon in *Staphylococcus aureus* and its regulation. *Int. J. Med. Microbiol.* **296,** 237–258 (2006).

98. Le, K. Y. & Otto, M. Quorum-sensing regulation in staphylococci-an overview. *Front. Microbiol.* **6,**

1174 (2015).

99. Lauderdale, K. J., Boles, B. R., Cheung, A. L. & Horswill, A. R. Interconnections between Sigma B, *agr*, and Proteolytic Activity in *Staphylococcus aureus* Biofilm Maturation. *Infect. Immun.* **77,** 1623–1635 (2009).

100. O'Callaghan, R. The Pathogenesis of *Staphylococcus aureus* Eye Infections. *Pathogens* **7,** 9 (2018).

101. Naber, C. K. *Staphylococcus aureus* Bacteremia: Epidemiology, Pathophysiology, and Management Strategies. *Clin. Infect. Dis.* **48,** S231–S237 (2009).

102. Wertheim, H. F. *et al.* The role of nasal carriage in *Staphylococcus aureus* infections. *Lancet Infect. Dis.* **5,** 751–762 (2005).

103. DeLeo, F. R., Otto, M., Kreiswirth, B. N. & Chambers, H. F. Community-associated meticillin-resistant *Staphylococcus aureus*. *Lancet* **375,** 1557–1568 (2010).

104. David, M. Z. & Daum, R. S. Community-associated methicillin-resistant *Staphylococcus aureus*: epidemiology and clinical consequences of an emerging epidemic. *Clin. Microbiol. Rev.* **23,** 616–87 (2010).

105. Peton, V. & Le Loir, Y. *Staphylococcus aureus* in veterinary medicine. *Infect. Genet. Evol.* **21,** 602–615 (2014).

106. Eriksen, K. R. 'Celbenin'-resistant staphylococci. *Ugeskr. Laeger* **123,** 384–6 (1961).

107. Jevons, M. P. 'Celbenin'-resistant Staphylococci. *BMJ* **1,** 124 (1961).

108. Eriksen, K. R. & Erichsen, I. Resistance to the Newer Penicillins. *BMJ* **1,** 746 (1963).

109. Hartman, B. & Tomasz, A. Altered penicillin-binding proteins in methicillin-resistant strains of *Staphylococcus aureus*. *Antimicrob. Agents Chemother.* **19,** 726–35 (1981).

110. Otto, M. Community-associated MRSA: What makes them special? *Int. J. Med. Microbiol.* **303,** 324–330 (2013).

111. Risson, D. C., O'Connor, E. D., Guard, R. W., Schooneveldt, J. M. & Nimmo, G. R. A fatal case of necrotising pneumonia due to community- associated methicillin-resistant *Staphylococcus aureus*. *Med. J. Aust. Med. J. Aust.* **186,** 479–480 (2007).

112. Iverson, A. R. *et al.* Influenza virus primes mice for pneumonia from *Staphylococcus aureus*. *J. Infect. Dis.* **203,** 880–888 (2011).

113. Montgomery, C. P. *et al.* Comparison of Virulence in Community-Associated Methicillin-Resistant *Staphylococcus aureus* Pulsotypes USA300 and USA400 in a Rat Model of Pneumonia. *J. Infect. Dis.* **198,** 561–570 (2008).

114. Harford, C. G., Smith, M. R. & Wood, W. B. Sulfonamide chemotherapy of combined infection with influenza virus and bacteria. *J. Exp. Med.* **83,** 505–18 (1946).

115. Lewis, P. A. & Shope, R. E. Swine influenza. *J. Exp. Med.* **54,** 361–71 (1931).

116. Masia, M. *et al.* Predictors of Pneumococcal Co-infection for Patients with Pandemic (H1N1) 2009 Influenza. *Emerg. Infect. Dis.* **17,** 1475–8 (2011).

117. Blyth, C. C. *et al.* The impact of bacterial and viral co-infection in severe influenza. *Influenza Other Respi. Viruses* **7,** 168–176 (2013).

118. Cillóniz, C. *et al.* Bacterial co-infection with H1N1 infection in patients admitted with community acquired pneumonia. *J. Infect.* **65,** 223–230 (2012).

119. Paddock, C. D. *et al.* Myocardial Injury and Bacterial Pneumonia Contribute to the Pathogenesis of Fatal Influenza B Virus Infection. *J. Infect. Dis.* **205,** 895–905 (2012).

120. Louria, D. B., Blumenfeld, H. L., Ellis, J. T., Kilbourne, E. D. & Rogers, D. E. Studies of influenza in the pandemic of 1957-1958. II. Pulmonary Complications of Influenza. *J. Clin. Invest.* **38,** 213–265 (1959).

121. Martin, C. M., Kunin, C. M., Gottlieb, L. S. & Finland, M. Asian influenza A in Boston, 1957-1958. II. Severe staphylococcal pneumonia complicating influenza. *AMA. Arch. Intern. Med.* **103,** 532–42 (1959).

122. Oseasohn, R., Adelson, L. & Kaji, M. Clinicopathologic Study of Thirty-Three Fatal Cases of Asian Influenza. *N. Engl. J. Med.* **260,** 509–518 (1959).

123. Hageman, J. C. *et al.* Severe community-acquired pneumonia due to *Staphylococcus aureus*, 2003-04 influenza season. *Emerg. Infect. Dis.* **12,** 894–9 (2006).

124. Trotter, Y. *et al.* Asian influenza in the United States, 1957-1958. *Am. J. Hyg.* **70,** 34–50 (1959).

125. Schwarzmann, S. W., Adler, J. L., Sullivan, R. J. & Marine, W. M. Bacterial pneumonia during the Hong Kong influenza epidemic of 1968-1969. *Arch. Intern. Med.* **127,** 1037–41 (1971).

126. Shieh, W.-J. *et al.* 2009 Pandemic Influenza A (H1N1). *Am. J. Pathol.* **177,** 166–175 (2010).

127. Monsalvo, A. C. *et al.* Severe pandemic 2009 H1N1 influenza disease due to pathogenic immune

complexes. *Nat. Med.* **17,** 195–199 (2011).

128. Morse, S. S. *et al.* Prediction and prevention of the next pandemic zoonosis. *Lancet* **380,** 1956–1965 (2012).

129. Löffler, B. *et al.* Pathogenesis of *Staphylococcus aureus* necrotizing pneumonia: the role of PVL and an influenza coinfection. *Expert Rev. Anti. Infect. Ther.* **11,** 1041–1051 (2013).

130. McAuley, J. L. *et al.* Expression of the 1918 Influenza A Virus PB1-F2 Enhances the Pathogenesis of Viral and Secondary Bacterial Pneumonia. *Cell Host Microbe* **2,** 240–249 (2007).

131. Hinshaw, V. S., Olsen, C. W., Dybdahl-Sissoko, N. & Evans, D. Apoptosis: a mechanism of cell killing by influenza A and B viruses. *J. Virol.* **68,** 3667–73 (1994).

132. Gamblin, S. J. & Skehel, J. J. Influenza hemagglutinin and neuraminidase membrane glycoproteins. *J. Biol. Chem.* **285,** 28403–9 (2010).

133. McCullers, J. A. The co-pathogenesis of influenza viruses with bacteria in the lung. *Nat. Rev. Microbiol.* **12,** 252–262 (2014).

134. Kash, J. C. *et al.* Lethal Synergism of 2009 Pandemic H1N1 Influenza Virus and *Streptococcus pneumoniae* Coinfection Is Associated with Loss of Murine Lung Repair Responses. *MBio* **2,** e00172-11-e00172-11 (2011).

135. Curtis, J. L. Pulmonary complications of oral-pharyngeal motility disorders. *GI Motil. online* (2006). doi:10.1038/gimo33

136. Blasi, F., Tarsia, P. & Aliberti, S. Strategic targets of essential host-pathogen interactions. *Respiration* **72,** 9–25 (2005).

137. Chaplin, D. D. Overview of the immune response. *J. Allergy Clin. Immunol.* **125,** S3-23 (2010).

138. Marks, L. R., Davidson, B. A., Knight, P. R. & Hakansson, A. P. Interkingdom signaling induces *Streptococcus pneumoniae* biofilm dispersion and transition from asymptomatic colonization to disease. *MBio* **4,** e00438-13 (2013).

139. Shrestha, S. *et al.* The role of influenza in the epidemiology of pneumonia. *Sci. Rep.* **5,** 15314 (2015).

140. McCullers, J. A. *et al.* Influenza Enhances Susceptibility to Natural Acquisition of and Disease due to *Streptococcus pneumoniae* in Ferrets. *J. Infect. Dis.* **202,** 1287–1295 (2010).

141. Mulcahy, M. E. & McLoughlin, R. M. *Staphylococcus aureus* and Influenza A Virus: Partners in Coinfection. *MBio* **7,** e02068-16 (2016).

142. Openshaw, P. J. Crossing barriers: infections of the lung and the gut. *Mucosal Immunol.* **2,** 100–102 (2009).

143. Lee, M. *et al.* A Postinfluenza Model of *Staphylococcus aureus* Pneumonia. *J. Infect. Dis.* **201,** 508–515 (2010).

144. Wallach, D., Kang, T.-B. & Kovalenko, A. Concepts of tissue injury and cell death in inflammation: a historical perspective. *Nat. Rev. Immunol.* **14,** 51–59 (2014).

145. Gilroy, D. & De Maeyer, R. New insights into the resolution of inflammation. *Semin. Immunol.* **27,** 161–168 (2015).

146. Rittirsch, D., Flierl, M. A. & Ward, P. A. Harmful molecular mechanisms in sepsis. *Nat. Rev. Immunol.* **8,** 776–787 (2008).

147. O'Shea, J. J., Ma, A. & Lipsky, P. Cytokines and autoimmunity. *Nat. Rev. Immunol.* **2,** 37–45 (2002).

148. Arango Duque, G. & Descoteaux, A. Macrophage cytokines: involvement in immunity and infectious diseases. *Front. Immunol.* **5,** 491 (2014).

149. McInnes, I. B. Cytokines. in *Kelley and Firestein's Textbook of Rheumatology* 396–407 (Elsevier, 2017).

150. Randall, R. E. & Goodbourn, S. Interferons and viruses: an interplay between induction, signalling, antiviral responses and virus countermeasures. *J. Gen. Virol.* **89,** 1–47 (2008).

151. Isaacs, A. & Lindenmann, J. Virus interference. I. The interferon. *Proc. R. Soc. London. Ser. B, Biol. Sci.* **147,** 258–67 (1957).

152. Goodbourn, S., Randall, R. E. & Didcock, L. Interferons: cell signalling, immune modulation, antiviral response and virus countermeasures. *J. Gen. Virol.* **81,** 2341–2364 (2000).

153. Tecchio, C., Micheletti, A. & Cassatella, M. A. Neutrophil-derived cytokines: facts beyond expression. *Front. Immunol.* **5,** 508 (2014).

154. Lacy, P. Editorial: secretion of cytokines and chemokines by innate immune cells. *Front. Immunol.* **6,** 190 (2015).

155. Zlotnik, A. & Yoshie, O. Chemokines: A New Classification Review System and Their Role in Immunity. *Immunity* **12,** 121–127 (2000).

156. Nomiyama, H., Osada, N. & Yoshie, O. Systematic classification of vertebrate chemokines based on conserved synteny and evolutionary history. *Genes to Cells* **18,** 1–16 (2013).

157. Griffith, J. W., Sokol, C. L. & Luster, A. D. Chemokines and Chemokine Receptors: Positioning Cells for Host Defense and Immunity. *Annu. Rev. Immunol.* **32,** 659–702 (2014).

158. Moser, B., Wolf, M., Walz, A. & Loetscher, P. Chemokines: multiple levels of leukocyte migration control. *Trends Immunol.* **25,** 75–84 (2004).

159. Thelen, M. Dancing to the tune of chemokines. *Nat. Immunol.* **2,** 129–134 (2001).

160. Wagner, M. J., Stacey, M. M., Liu, B. A. & Pawson, T. Molecular Mechanisms of SH2- and PTB-Domain-Containing Proteins in Receptor Tyrosine Kinase Signaling. *Cold Spring Harb. Perspect. Biol.* **5,** a008987–a008987 (2013).

161. Liongue, C., O'Sullivan, L. A., Trengove, M. C. & Ward, A. C. Evolution of JAK-STAT Pathway Components: Mechanisms and Role in Immune System Development. *PLoS One* **7,** e32777 (2012).

162. O'Shea, J. J. *et al.* The JAK-STAT Pathway: Impact on Human Disease and Therapeutic Intervention. *Annu. Rev. Med* **66,** 311–28 (2015).

163. Seif, F. *et al.* The role of JAK-STAT signaling pathway and its regulators in the fate of T helper cells. *Cell Commun. Signal.* **15,** 23 (2017).

164. Yamaoka, K. *et al.* The Janus kinases (Jaks). *Genome Biol.* **5,** 253 (2004).

165. Babon, J. J., Lucet, I. S., Murphy, J. M., Nicola, N. A. & Varghese, L. N. The molecular regulation of Janus kinase (JAK) activation. *Biochem. J* **462,** 1–13 (2014).

166. Nardozzi, J. D., Lott, K. & Cingolani, G. Phosphorylation meets nuclear import: a review. *Cell Commun. Signal.* **8,** 32 (2010).

167. O'Shea, J. J. & Murray, P. J. Cytokine Signaling Modules in Inflammatory Responses. *Immunity* **28,** 477–487 (2008).

168. Rawlings, J. S., Rosler, K. M. & Harrison, D. A. The JAK/STAT signaling pathway. *J. Cell Sci.* **117,** 1281–1283 (2004).

169. Khodarev, N. N., Roizman, B. & Weichselbaum, R. R. Molecular Pathways: Interferon/Stat1 Pathway: Role in the Tumor Resistance to Genotoxic Stress and Aggressive Growth. *Clin. Cancer Res.* **18,** 3015–3021 (2012).

170. Schindler, C., Fu, X. Y., Improta, T., Aebersold, R. & Darnell, J. E. Proteins of transcription factor ISGF-3: one gene encodes the 91-and 84-kDa ISGF-3 proteins that are activated by interferon alpha. *Proc. Natl. Acad. Sci. U. S. A.* **89,** 7836–9 (1992).

171. Zhang, Y. *et al.* STAT1β enhances STAT1 function by protecting STAT1α from degradation in esophageal squamous cell carcinoma. *Cell Death Dis.* **8,** 3077 (2017).

172. Najjar, I. & Fagard, R. STAT1 and pathogens, not a friendly relationship. *Biochimie* **92,** 425–444 (2010).

173. Koromilas, A. E. & Sexl, V. The tumor suppressor function of STAT1 in breast cancer. *JAK-STAT* **2,** e23353 (2013).

174. Meraz, M. A. *et al.* Targeted disruption of the Stat1 gene in mice reveals unexpected physiologic specificity in the JAK-STAT signaling pathway. *Cell* **84,** 431–42 (1996).

175. Durbin, J. E., Hackenmiller, R., Simon, M. C. & Levy, D. E. Targeted disruption of the mouse Stat1 gene results in compromised innate immunity to viral disease. *Cell* **84,** 443–50 (1996).

176. Chapgier, A. *et al.* Novel STAT1 Alleles in Otherwise Healthy Patients with Mycobacterial Disease. *PLoS Genet.* **2,** e131 (2006).

177. Dupuis, S. *et al.* Impaired response to interferon-α/β and lethal viral disease in human STAT1 deficiency. *Nat. Genet.* **33,** 388–391 (2003).

178. Russell-Harde, D. *et al.* Reconstitution of a high affinity binding site for type I interferons. *J. Biol. Chem.* **270,** 26033–6 (1995).

179. Cohen, B., Novick, D., Barak, S. & Rubinstein, M. Ligand-induced association of the type I interferon receptor components. *Mol. Cell. Biol.* **15,** 4208–14 (1995).

180. Gauzzi, M. C. *et al.* Interferon-alpha-dependent activation of Tyk2 requires phosphorylation of positive regulatory tyrosines by another kinase. *J. Biol. Chem.* **271,** 20494–500 (1996).

181. Krishnan, K., Yan, H., Lim, J. T. & Krolewski, J. J. Dimerization of a chimeric CD4-interferon-alpha receptor reconstitutes the signaling events preceding STAT phosphorylation. *Oncogene* **13,** 125–33 (1996).

182. Greenlund, A. C. *et al.* Stat recruitment by tyrosine-phosphorylated cytokine receptors: an ordered reversible affinity-driven process. *Immunity* **2,** 677–87 (1995).

183. Heim, M. H., Kerr, I. M., Stark, G. R. & Darnell, J. E. Contribution of STAT SH2 groups to specific interferon signaling by the Jak-STAT pathway. *Science* **267,** 1347–9 (1995).

184. Shuai, K. *et al.* Interferon activation of the transcription factor Stat91 involves dimerization through SH2-phosphotyrosyl peptide interactions. *Cell* **76,** 821–8 (1994).

185. Darnell, J. E., Kerr, I. M. & Stark, G. R. Jak-STAT pathways and transcriptional activation in response to IFNs and other extracellular signaling proteins. *Science* **264,** 1415–21 (1994).

186. Steen, H. C. & Gamero, A. M. STAT2 phosphorylation and signaling. *JAK-STAT* **2,** e25790 (2013).

187. Au-Yeung, N., Mandhana, R. & Horvath, C. M. Transcriptional regulation by STAT1 and STAT2 in the interferon JAK-STAT pathway. *JAK-STAT* **2,** e23931 (2013).

188. Min, J.-Y. & Krug, R. M. The primary function of RNA binding by the influenza A virus NS1 protein in infected cells: Inhibiting the 2'-5' oligo (A) synthetase/RNase L pathway. *Proc. Natl. Acad. Sci.* **103,** 7100–7105 (2006).

189. Satterly, N. *et al.* Influenza virus targets the mRNA export machinery and the nuclear pore complex. *Proc. Natl. Acad. Sci.* **104,** 1853–1858 (2007).

190. Dudek, S. E. *et al.* The influenza virus PB1-F2 protein has interferon antagonistic activity. *Biol. Chem.* **392,** 1135–44 (2011).

191. Varga, Z. T. *et al.* The Influenza Virus Protein PB1-F2 Inhibits the Induction of Type I Interferon at the Level of the MAVS Adaptor Protein. *PLoS Pathog.* **7,** e1002067 (2011).

192. Liedmann, S. *et al.* New Virulence Determinants Contribute to the Enhanced Immune Response and Reduced Virulence of an Influenza A Virus A/PR8/34 Variant. *J. Infect. Dis.* **209,** 532–541 (2014).

193. Graef, K. M. *et al.* The PB2 Subunit of the Influenza Virus RNA Polymerase Affects Virulence by Interacting with the Mitochondrial Antiviral Signaling Protein and Inhibiting Expression of Beta Interferon. *J. Virol.* **84,** 8433–8445 (2010).

194. Hui, K. P. Y. *et al.* Induction of proinflammatory cytokines in primary human macrophages by influenza A virus (H5N1) is selectively regulated by IFN regulatory factor 3 and p38 MAPK. *J. Immunol.* **182,** 1088–98 (2009).

195. Perrone, L. A., Plowden, J. K., García-Sastre, A., Katz, J. M. & Tumpey, T. M. H5N1 and 1918 Pandemic Influenza Virus Infection Results in Early and Excessive Infiltration of Macrophages and Neutrophils in the Lungs of Mice. *PLoS Pathog.* **4,** e1000115 (2008).

196. La Gruta, N. L., Kedzierska, K., Stambas, J. & Doherty, P. C. A question of self-preservation: immunopathology in influenza virus infection. *Immunol. Cell Biol.* **85,** 85–92 (2007).

197. Taubenberger, J. K. & Morens, D. M. The Pathology of Influenza Virus Infections. *Annu. Rev. Pathol. Mech. Dis.* **3,** 499–522 (2008).

198. LeBouder, E. *et al.* Soluble forms of Toll-like receptor (TLR)2 capable of modulating TLR2 signaling are present in human plasma and breast milk. *J. Immunol.* **171,** 6680–9 (2003).

199. Gay, N. J. & Gangloff, M. Structure and Function of Toll Receptors and Their Ligands. *Annu. Rev. Biochem.* **76,** 141–165 (2007).

200. Kaisho, T. & Akira, S. Toll-like receptor function and signaling. *J. Allergy Clin. Immunol.* **117,** 979–987 (2006).

201. Bekeredjian-Ding, I., Stein, C. & Uebele, J. The Innate Immune Response Against *Staphylococcus aureus*. in *Staphylococcus aureus* 385–418 (Springer, Cham, 2015).

202. Boxx, G. M. & Cheng, G. The Roles of Type I Interferon in Bacterial Infection. *Cell Host Microbe* **19,** 760–769 (2016).

203. Martin, F. J. *et al. Staphylococcus aureus* activates type I IFN signaling in mice and humans through the Xr repeated sequences of protein A. *J. Clin. Invest.* **119,** 1931–9 (2009).

204. Hultgren, O. H., Stenson, M. & Tarkowski, A. Role of IL-12 in *Staphylococcus aureus*-triggered arthritis and sepsis. *Arthritis Res.* **3,** 41–7 (2001).

205. Nakane, A., Okamoto, M., Asano, M., Kohanawa, M. & Minagawa, T. Endogenous Gamma Interferon, Tumor Necrosis Factor, and Interleukin-6 in *Staphylococcus aureus* Infection in Mice. *Infect. Immun.* **63,** 1165–1172 (1995).

206. Karlström, Å., Heston, S. M., Boyd, K. L., Tuomanen, E. I. & McCullers, J. A. Toll-Like Receptor 2 Mediates Fatal Immunopathology in Mice During Treatment of Secondary Pneumococcal Pneumonia Following Influenza. *J. Infect. Dis.* **204,** 1358–1366 (2011).

207. Warnking, K. *et al.* Super-infection with *Staphylococcus aureus* inhibits influenza virus-induced type I IFN signalling through impaired STAT1-STAT2 dimerization. *Cell. Microbiol.* **17,** 303–317 (2015).

208. Tuchscherr, L. *et al. Staphylococcus aureus* phenotype switching: an effective bacterial strategy to escape host immune response and establish a chronic infection. *EMBO Mol. Med.* **3,** 129–41 (2011).

209. Schmolke, M., Viemann, D., Roth, J. & Ludwig, S. Essential impact of NF-κB signaling on the H5N1 influenza A virus-induced transcriptome. *J. Immunol.* **183,** 5180–9 (2009).

210. Richt, J. A. *et al.* Real–Time Reverse Transcription–Polymerase Chain Reaction Assays for the Detection and Differentiation of North American Swine Influenza Viruses. *J. Vet. Diagnostic Investig.* **16,** 367–373 (2004).

211. Horsburgh, M. J. *et al.* sigmaB modulates virulence determinant expression and stress resistance: characterization of a functional *rsbU* strain derived from *Staphylococcus aureus* 8325-4. *J. Bacteriol.* **184,** 5457–67 (2002).

212. Werdan, K. *et al.* Mechanisms of infective endocarditis: pathogen–host interaction and risk states. *Nat. Rev. Cardiol.* **11,** 35–50 (2014).

213. Lew, D. P. & Waldvogel, F. A. Osteomyelitis. *Lancet* **364,** 369–379 (2004).

214. Bradford, M. M. A rapid and sensitive method for the quantitation of microgram quantities of protein utilizing the principle of protein-dye binding. *Anal. Biochem.* **72,** 248–54 (1976).

215. Livak, K. J. & Schmittgen, T. D. Analysis of Relative Gene Expression Data Using Real-Time Quantitative PCR and the $2^{-\Delta\Delta C_T}$ Method. *Methods* **25,** 402–408 (2001).

216. Li, X., Leung, S., Qureshi, S., Darnell, J. E. & Stark, G. R. Formation of STAT1-STAT2 heterodimers and their role in the activation of IRF-1 gene transcription by interferon-alpha. *J. Biol. Chem.* **271,** 5790–4 (1996).

217. Ghislain, J. J., Wong, T., Nguyen, M. & Fish, E. N. The Interferon-Inducible Stat2:Stat1 Heterodimer Preferentially Binds *In Vitro* to a Consensus Element Found in the Promoters of a Subset of Interferon-Stimulated Genes. *J. Interf. Cytokine Res.* **21,** 379–388 (2001).

218. Klemm, C. *et al.* Mitogen-activated protein kinases (MAPKs) regulate IL-6 over-production during concomitant influenza virus and *Staphylococcus aureus* infection. *Sci. Rep.* **7,** 42473 (2017).

219. Strobel, M. *et al.* Post-invasion events after infection with *Staphylococcus aureus* are strongly dependent on both the host cell type and the infecting *S. aureus* strain. *Clin. Microbiol. Infect.* **22,** 799–809 (2016).

220. Short, K. R. *et al.* Influenza virus damages the alveolar barrier by disrupting epithelial cell tight junctions. *Eur. Respir. J.* **47,** 954–66 (2016).

221. Bremell, T. *et al.* Outbreak of spontaneous staphylococcal arthritis and osteitis in mice. *Arthritis Rheum.* **33,** 1739–44 (1990).

222. Bremell, T., Abdelnour, A. & Tarkowski, A. Histopathological and serological progression of experimental *Staphylococcus aureus* arthritis. *Infect. Immun.* **60,** 2976–85 (1992).

223. Queck, S. Y. *et al.* RNAIII-Independent Target Gene Control by the agr Quorum-Sensing System: Insight into the Evolution of Virulence Regulation in *Staphylococcus aureus*. *Mol. Cell* **32,** 150–158 (2008).

224. Narasaraju, T. *et al.* Adaptation of human influenza H3N2 virus in a mouse pneumonitis model: insights into viral virulence, tissue tropism and host pathogenesis. *Microbes Infect.* **11,** 2–11 (2009).

225. Holtfreter, S. *et al.* Characterization of a Mouse-Adapted *Staphylococcus aureus* Strain. *PLoS One* **8,** e71142 (2013).

226. Guinane, C. M. *et al.* Evolutionary Genomics of *Staphylococcus aureus* Reveals Insights into the Origin and Molecular Basis of Ruminant Host Adaptation. *Genome Biol. Evol.* **2,** 454–466 (2010).

227. Herron-Olson, L., Fitzgerald, J. R., Musser, J. M. & Kapur, V. Molecular Correlates of Host Specialization in *Staphylococcus aureus*. *PLoS One* **2,** e1120 (2007).

228. He, L. *et al.* Detection and analysis of methicillin-resistant human-adapted sequence type 398 allows insight into community-associated methicillin-resistant *Staphylococcus aureus* evolution. *Genome Med.* **10,** 5 (2018).

229. Waters, C. M. & Bassler, B. L. Quorum sensing: Cell-to-Cell communication in bacteria. *Annu. Rev. Cell Dev. Biol.* **21,** 319–346 (2005).

230. Cegelski, L., Marshall, G. R., Eldridge, G. R. & Hultgren, S. J. The biology and future prospects of antivirulence therapies. *Nat. Rev. Microbiol.* **6,** 17–27 (2008).

231. Dufour, P. *et al.* High genetic variability of the *agr* locus in *Staphylococcus* species. *J. Bacteriol.* **184,** 1180–6 (2002).

232. Recker, M. *et al.* Clonal differences in *Staphylococcus aureus* bacteraemia-associated mortality. *Nat. Microbiol.* **2,** 1381–1388 (2017).

233. Traber, K. E. *et al. agr* function in clinical *Staphylococcus aureus* isolates. *Microbiology* **154,** 2265–2274 (2008).

234. Smyth, D. S. *et al.* Nasal Carriage as a Source of *agr*-Defective *Staphylococcus aureus* Bacteremia. *J. Infect. Dis.* **206,** 1168–1177 (2012).

235. Painter, K. L., Krishna, A., Wigneshweraraj, S. & Edwards, A. M. What role does the quorum-sensing accessory gene regulator system play during *Staphylococcus aureus* bacteremia? *Trends Microbiol.* **22,** 676–685 (2014).

236. Suligoy, C. M. *et al.* Mutation of *Agr* Is Associated with the Adaptation of *Staphylococcus aureus* to the Host during Chronic Osteomyelitis. *Front. Cell. Infect. Microbiol.* **8,** 18 (2018).

237. Ferreira, F. A. *et al.* Impact of *agr* dysfunction on virulence profiles and infections associated with a

novel methicillin-resistant *Staphylococcus aureus* (MRSA) variant of the lineage ST1-SCC*mec* IV. *BMC Microbiol.* **13,** 93 (2013).

238. Chong, Y. P. *et al.* Accessory gene regulator (*agr*) dysfunction in *Staphylococcus aureus* bloodstream isolates from South Korean patients. *Antimicrob. Agents Chemother.* **57,** 1509–12 (2013).

239. Schwan, W. R., Langhorne, M. H., Ritchie, H. D. & Stover, C. K. Loss of hemolysin expression in *Staphylococcus aureus agr* mutants correlates with selective survival during mixed infections in murine abscesses and wounds. *FEMS Immunol. Med. Microbiol.* **38,** 23–8 (2003).

240. Savage, V. J., Chopra, I. & O'Neill, A. J. Population Diversification in *Staphylococcus aureus* Biofilms May Promote Dissemination and Persistence. *PLoS One* **8,** e62513 (2013).

241. Beenken, K. E. *et al.* Epistatic Relationships between *sarA* and *agr* in *Staphylococcus aureus* Biofilm Formation. *PLoS One* **5,** e10790 (2010).

242. Gresham, H. D. *et al.* Survival of *Staphylococcus aureus* inside neutrophils contributes to infection. *J. Immunol.* **164,** 3713–22 (2000).

243. Kubica, M. *et al.* A Potential New Pathway for *Staphylococcus aureus* Dissemination: The Silent Survival of *S. aureus* Phagocytosed by Human Monocyte-Derived Macrophages. *PLoS One* **3,** e1409 (2008).

244. Voyich, J. M. *et al.* Insights into mechanisms used by *Staphylococcus aureus* to avoid destruction by human neutrophils. *J. Immunol.* **175,** 3907–19 (2005).

245. Alexander, E. H. & Hudson, M. C. Factors influencing the internalization of *Staphylococcus aureus* and impacts on the course of infections in humans. *Appl. Microbiol. Biotechnol.* **56,** 361–6 (2001).

246. Löffler, B., Tuchscherr, L., Niemann, S. & Peters, G. *Staphylococcus aureus* persistence in non-professional phagocytes. *Int. J. Med. Microbiol.* **304,** 170–176 (2014).

247. Hoffmann, J. *et al.* Viral and bacterial co-infection in severe pneumonia triggers innate immune responses and specifically enhances IP-10: a translational study. *Sci. Rep.* **6,** 38532 (2016).

248. Kj, C. *et al.* Respiratory Syncytial Virus Infection is Associated with Increased Bacterial Load in the Upper Respiratory Tract in Young Children. *J Med. Microbiol Diagnosis* 1 (2013). doi:10.4172/2161-0703.S1-005

249. Ballinger, M. N. & Standiford, T. J. Postinfluenza bacterial pneumonia: host defenses gone awry. *J. Interf. cytokine Res.* **30,** 643–52 (2010).

250. D'Anna, S. E., Balbi, B., Cappello, F., Carone, M. & Di Stefano, A. Bacterial-viral load and the immune response in stable and exacerbated COPD: significance and therapeutic prospects. *Int. J. Chron. Obstruct. Pulmon. Dis.* **11,** 445–53 (2016).

251. Shigeishi, H. *et al.* High HPV16 E6 viral load in the oral cavity is associated with an increased number of bacteria: A preliminary study. *Biomed. Reports* **8,** 59–64 (2017).

252. Oda, K. *et al.* Structural analysis of the STAT1:STAT2 heterodimer revealed the mechanism of Sendai virus C protein-mediated blockade of type 1 interferon signaling. *J. Biol. Chem.* **292,** 19752–19766 (2017).

253. Kato, A. *et al.* Y2, the smallest of the Sendai virus C proteins, is fully capable of both counteracting the antiviral action of interferons and inhibiting viral RNA synthesis. *J. Virol.* **75,** 3802–10 (2001).

254. Shahangian, A. *et al.* Type I IFNs mediate development of postinfluenza bacterial pneumonia in mice. *J. Clin. Invest.* **119,** 1910–20 (2009).

255. Lee, B. *et al.* STAT1 Is Required for Suppression of Type 17 Immunity during Influenza and Bacterial Superinfection. *ImmunoHorizons* **1,** 81–91 (2017).

256. Amadi-Obi, A. *et al.* TH17 cells contribute to uveitis and scleritis and are expanded by IL-2 and inhibited by IL-27/STAT1. *Nat. Med.* **13,** 711–718 (2007).

257. Guo, B., Chang, E. Y. & Cheng, G. The type I IFN induction pathway constrains Th17-mediated autoimmune inflammation in mice. *J. Clin. Invest.* **118,** 1680–90 (2008).

258. Parker, D. Impact of Type I and III Interferons on Respiratory Superinfections Due to Multidrug-Resistant Pathogens. *J. Infect. Dis.* **215,** S58–S63 (2017).

259. Prinz, M. *et al.* Distinct and Nonredundant In Vivo Functions of IFNAR on Myeloid Cells Limit Autoimmunity in the Central Nervous System. *Immunity* **28,** 675–686 (2008).

260. Yarilina, A., Park-Min, K.-H., Antoniv, T., Hu, X. & Ivashkiv, L. B. TNF activates an IRF1-dependent autocrine loop leading to sustained expression of chemokines and STAT1-dependent type I interferon–response genes. *Nat. Immunol.* **9,** 378–387 (2008).

261. Durbin, J. E. *et al.* Type I IFN modulates innate and specific antiviral immunity. *J. Immunol.* **164,** 4220–8 (2000).